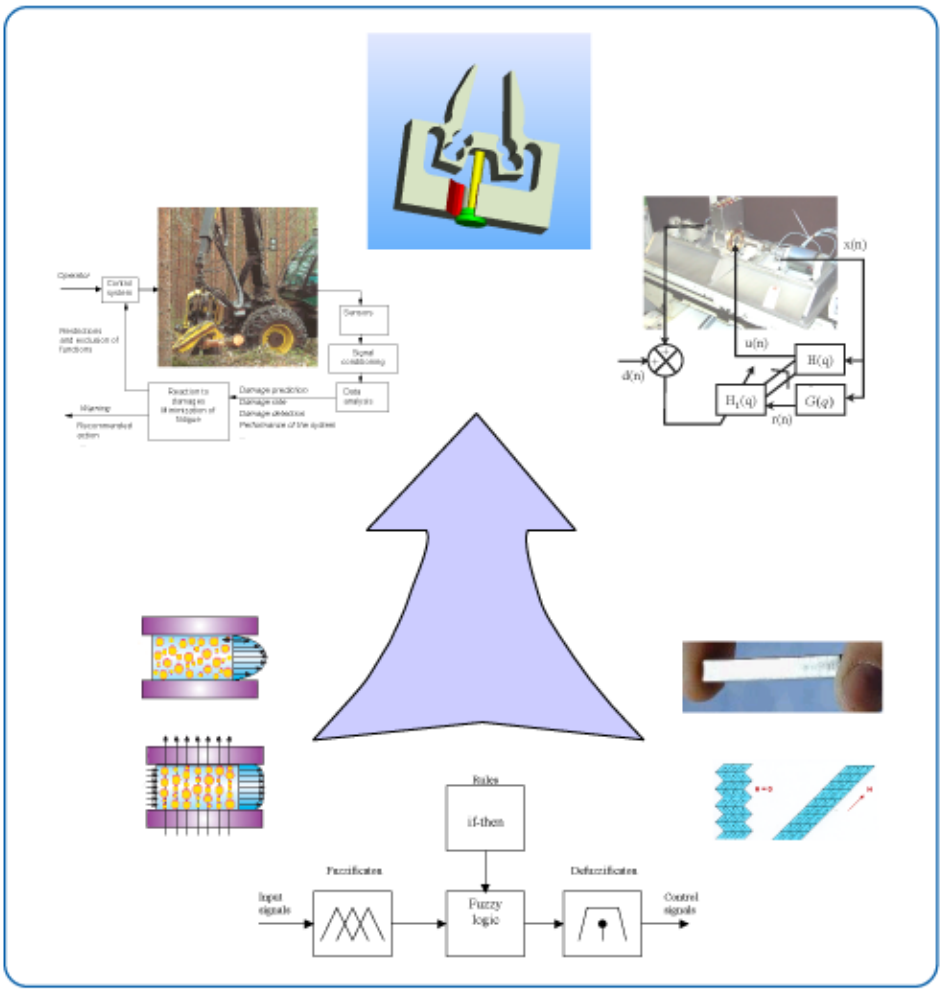

Smart materials and structures

VTT Research Programme 2000–2002

VTT SYMPOSIUM 225

Keywords: adaptronics, smart materials, smart structures, intelligent systems, multifunctional systems, adaptive systems, vibration control, durability control, active materials, active control, semi-active control

Smart materials and structures

VTT Research Program 2000–2002

Espoo, Finland, 4th December, 2002

Edited by

Ismo Vessonen

VTT Industrial Systems

Organised by

VTT Industrial Systems

ISBN 951–38–6278–X (soft back ed.)
ISSN 0357–9387 (soft back ed.)

ISBN 951–38–6279–8 (URL:http://www.inf.vtt.fi/pdf/)
ISSN 1455–0873 (URL: http://www.inf.vtt.fi/pdf/)

JULKAISIJA – UTGIVARE – PUBLISHER

VTT, Vuorimiehentie 5, PL 2000, 02044 VTT
puh. vaihde (09) 4561, faksi 456 4374

VTT, Bergsmansvägen 5, PB 2000, 02044 VTT
tel. växel (09) 4561, fax 456 4374

VTT Technical Research Centre of Finland
Vuorimiehentie 5, P.O.Box 2000, FIN–02044 VTT, Finland
phone (internat.) + 358 9 4561, fax + 358 9 456 4374

VTT Tuotteet ja tuotanto, Otakaari 7 B, PL 13022, 02044 VTT
puh. vaihde (09) 4561, faksi (09) 456 6475

VTT Industriella System, Otsvängen 7 B, PB 13022, 02044 VTT
tel. växel (09) 4561, fax (09) 456 6475

VTT Industrial Systems, Otakaari 7 B, P.O.Box 13022, FIN–02044 VTT, Finland
phone internat. + 358 9 4561, fax + 358 9 456 6475

Technical editing Leena Ukskoski

Otamedia Oy, Espoo 2003

Preface

This publication documents the presentations given at the closing seminar of the "Smart Materials and Structures" (Älykkäät materiaalit ja rakenteet, ÄLYMARA) technology program on December 4th 2002 at Otaniemi, Espoo. The purpose of the seminar was to summarise and present, to VTT´s researchers and invited representatives of industry, the research work and technical results done and achieved in the four subprojects "Active materials", "Precision motion and force", "Active durability control", and "Active vibration control" of the program. ÄLYMARA (2000–2002) was an internal research effort of VTT Industrial Systems entirely funded by VTT.

The trend in technology development is towards multifunctional and, at the same time user-friendly, smart or intelligent products with the ability to continuously monitor their internal status and the external environment. These products should automatically adapt to environmental and operational conditions, maintain optimal performance in variable circumstances including exceptional cases, and actively communicate with the user, environment and/or with other products and systems.

The implementation of multifunctional smart structures and systems requires know-how in several technologies, e.g., active materials, structural mechanics, micro-sensors, signal analysis, control technology, soft computing, wireless communication, functional virtual prototyping etc. The aim of the program was mainly to develop expertise on how to integrating these new technologies into the basic knowledge of different application areas and the physical phenomena within them, in order to create new innovative technical solutions. The long-term goal of the research work is to be able to apply the know-how to intelligent products so as to support R&D efforts and the competitive edge of Finnish industry.

The program team wish to thank the steering group and all the participated research personnel for creating an open and comfortable, but at the same time progress-oriented atmosphere for the program. The help and expert views of R. Hedman Emmecon Ltd, J.-P. Hyvärinen Univ. of Oulu, H. Kylmälä Univ. of Oulu, E. Lantto High Speed Tech Ltd, K. Nevala Univ. of Oulu and A. Vähänikkilä Univ. of Oulu is also greatly appreciated.

Espoo, December, 2002 Ismo Vessonen

Contents

Smart Materials

Marke Kallio[1)], Reima Lahtinen[2)], Jari Koskinen[2)]
[1)]VTT Processes, Tampere, Finland
[2)]VTT Industrial Systems, Espoo, Finland

Abstract

The field of smart materials and structures is emerging rapidly with technological innovations appearing in engineering materials, sensors, actuators and image processing. Smart materials can be defined in several ways [1]:

1. Materials functioning as both sensing and actuating
2. Materials, which have multiple responses to one stimulus in a coordinated fashion
3. Passively smart materials with self-repairing or stand-by characteristics to withstand sudden changes
4. Actively smart materials utilising feedback
5. Smart materials and systems reproducing biological functions in load bearing systems.

Smart materials can be either inorganic, organic or composites. In this article, different groups of smart materials are presented and their properties are discussed.

1. Piezoelectric ceramics

1.1 Materials

The first piezoelectric ceramics were single crystals. However, polycrystalline ceramics have several advantages over single crystals, including higher

sensitivity and ease of fabrication into a variety of shapes and sizes. The crystal structure of a material changes at the Curie temperature (T_C), from piezoelectric (asymmetrical) to a non-piezoelectric (symmetrical) form. A peak in the dielectric constant and a complete loss of all piezoelectric properties accompanies this phase change [41].

The most commonly used piezoelectric ceramics are barium titanate ($BaTiO_3$), lead zirconate titanate PZT ($PbZrTiO_3$) and lead lanthanum zirconate titanate PLZT. These materials exhibit nonlinear coupling between a mechanical and an electric response. They undergo spontaneous polarisation at temperatures below the Curie temperature and when under the electric field, either domain switching or phase transformation is achieved. Piezoelectric ceramics can be either monolithic or made of thin, stacked ceramic layers. The common feature of stacked actuators and benders is that many thin layers of piezoelectric material are glued or cofired together with an electrode between each layer. The thickness of the layers is usually 30–200 μm. This leads to large displacements; 0.2 % strain with lower voltage levels than would be achievable with a monolithic element of the same length [41].

1.2 Properties

Piezoactuators are high-force, but low stroke devices. The strain of these materials is relatively small but the specific actuation stress and the bandwidth can be very high [2]. Piezoelectric materials exhibit a mechanical hysteresis, which depends on the material and can range from 4 to 30%.

The piezoelectric properties are dependent on temperature. Maximum application temperatures can be as high as 300°C but should not exceed the Curie temperature of the material. A problem of heat dissipation is associated with piezoelectric material. The system dissipative power is eventually transformed into internal heat energy. Overvoltage and current should be avoided when using piezoelectric materials. Exceeding the driving voltage limits can cause deterioration or depolarisation of material. Actuators are often used in dynamic conditions, which means that depending on operating frequency and cooling conditions it may be necessary to reduce the voltage amplitude to less than the V_{max} recommended.

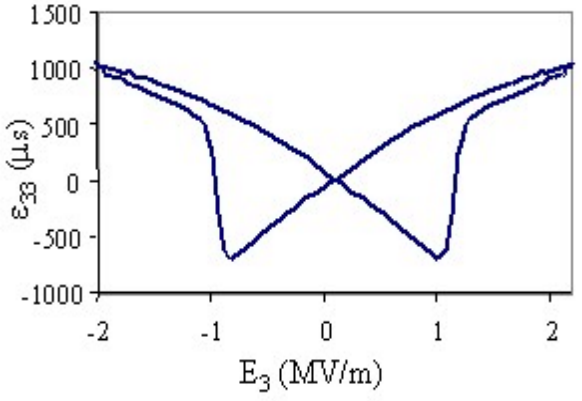

Figure 1. When electric field is applied opposite to the polarisation direction, the material undergoes 180º switching, producing characteristic strain-electric field butterfly loop and flux-electric field hysteresis curves [40].

1.3 Applications

Piezoelectric materials are currently being considered for a number of actuator applications including precision positioning, vibration suppression, noise control and inkjet printing. Piezoelectric actuators have been used for the active shape, vibration and acoustic control of structures. Their ability to be easily integrated into structures makes them very attractive in structural control. Multilayer actuators have advantages such as fast switching time, high blocking force and low driving voltage. These features can be utilised in, for example, the automotive area for fast injection valves, accelerometers or in the textile industry for automated weaver's looms [1, 3]. A few applications are listed below [41]:

- Acoustic emission transducers, alarm systems: movement detectors, window sensors
- Flow meters: blood, industrial processes, waste water
- Hydrophones: seismic, biologic, military, underwater communication
- Industrial sensors based on ultrasound: level control, detection, identification, medical: scanning, heat treatment, surgical knives, cleaning of veins

- Micro positioning devices: optics, scanning tunnelling microscopes
- SAW: surface acoustic waves. personal computer touch screens, filters
- Welding and drilling of metals and plastics.

Stacked actuators have been used in applications included micro-positioning, vibration isolation, fast acting valves and nozzles, transducers and gas igniters. They have also been utilised for shock absorption in luxury cars, spacecraft jitter reduction and active engine mounts [1].

1.4 Piezoelectric composites

Active material interaction with other materials such as polymers and composites is the basis for many applications in actuator integration in smart structures. Noise reduction by using additional damping material is associated with a higher structural weight. Piezoelectric ceramics seem to be the most promising materials for automobile structures because of their high manipulating speed and their accuracy.

Active Fiber Composites (AFCs) have been successfully developed at MIT to address the most critical properties restricting the use of piezoelectric materials: brittleness, limited robustness, limited conformability and in-plane actuation isotropy. AFCs consist of small semi-continuous piezoelectric fibers uniaxially aligned in a polymer matrix (epoxy) between two interdigitated electrodes. Each fiber is surrounded and protected by the polymer matrix. These actuators can be used in, for example, active helicopter rotor blades or in the active control of acoustics [6].

2. Shape memory alloys

2.1 Definition

A Shape Memory Alloy (SMA) is an alloy which, when deformed (in the martensitic phase) with the external stresses removed and then heated, will

regain its original "memory" shape (in the austenitic phase). Shape memory alloys can thus transform thermal energy directly to mechanical work. The characteristic transformation temperatures are defined as follows [9, 10]:

M_s: martensite start temperature upon cooling

M_f: martensite finish temperature upon cooling

A_s: reverse transformation start temperature upon heating

A_f: reverse transformation finish temperature upon heating.

The thermoelastic martensite transformations are characterised by a small hysteresis between the starting temperature of transformation (M_s) and its reverse (A_s), and the continuous growth of the martensite. The usual way of characterising the transformation and naming each point in the cycle is shown in Fig. 2. The transformation also exhibits hysteresis. This transformation hysteresis (shown as T_1 in Fig. 2) varies with the alloy system [7, 17, 43].

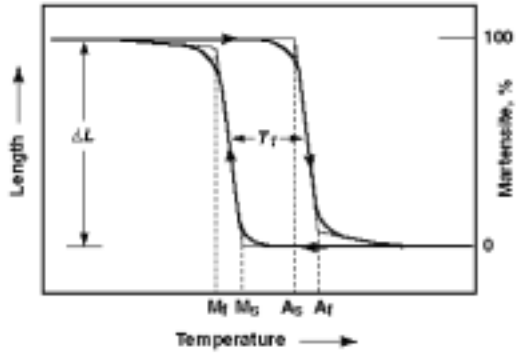

Figure 2. The typical temperature-transformation curve of a NiTi alloy [43].

The superelasticity (SE) effect is common for SMA intermetallics. SE, which is a pseudoelasticity occurring at a temperature above A_f (slightly above their transformation temperatures). This provides a very springy, "rubberlike" elasticity in these alloys. SMA is a natural smart material, i.e., 1) sensor (thermal), 2) actuator (shape memory deformation) and 3) memory and shape recovery [9].

2.2 Materials

The best known SMAs are the nickel-titanium alloys named Nitinol and Flexinol. Other metallic materials that are known to exhibit shape memory effect include the copper alloy systems Cu-Zn, Cu-Zn-Al, Cu-Zn-Ga, Cu-Zn-Sn, Cu-Zn-Si, Cu-Al-Ni, Cu-Au-Zn, Cu-Sn, and the alloys of Au-Cd, Ni-Al, Fe-Pt, etc. The newly developed FeMnSiCrNi shape memory stainless steels (SMSS) have attracted substantial interest because of their good shape memory effect, mechanical properties, machinability, weldability and corrosion resistance [7].

2.3 Properties

SMAs are highly adaptive, compact, lightweight and have a high force-to-weight ratio. SMAs are the only materials that can impart both large strains and large forces but their poor energy conversion remains a problem [1, 2]. In dynamic applications, which require heating and cooling of the wires to start and stop the recovery process, the heating and cooling rates become a limiting factor. Electric heating can drive the transformation, while cooling depends on heat conduction, which is a slow process for many applications. The frequency is therefore small; at best 3 Hz has been achieved [1, 2].

The superelastic Nitinol's flexibility is 10–20 times greater than that of stainless steel; that is to say, one can observe devices "springback" with strains as high as 11%. The Nitinol is also biocompatible and MR compatible, which means several possible uses in medicine [11].

SMA wires that are 37 to 375 μm across will respond quickly enough to move objects within about 1 second, yet still exert forces up to 20 N. Costs and size requirements are low, reliabilities high and energy requirements acceptable. Applications being researched range from remote-controlled valves to walking robots capable of detonating mines.

2.4 Degradation and fatigue

The reliability of a SM device depends on its global lifetime performance. Time, temperature, stress, transformation strain and the amount of transformation cycles are the important controlling external parameters. The important internal parameters that determine the physical and mechanical properties are the alloy system, the alloy composition, the type of transformation and the lattice structure, including defects. These parameters are controlled by the thermo-mechanical history of the alloy [12].

As a consequence, the maximum memory effect, strain and/or stress, will be restricted depending on the required amount of cycles. In the following table the relation between the envisaged amount of cycles and allowed maximum strain and stress is given for Ni-Ti alloy [12].

2.5 Applications

The application areas of SM alloys include both shape memory (SM) and superelastic (SE) usages [12]:

- SE: medical applications *(stents, joints)* fashion, decoration and gadgets *(spectacle frames, bra frames, antennas for cellular phones, headbands for headphones (Sony minidisc), shutable lamp shades)*
- SM: couplings and fasteners *(heat-recoverable couplings (Raychem), heat-to-shrink fasteners, dematable connectors)*
- SM: (micro-) actuators *(thermostats, valves, positioners, grippers, pumps, release mechanics, robots)*
- SM: adaptive materials and hybrid composites, applications based on the high damping capacity of SMA.

Sputter-deposited Ni-Ti films are regarded as prospective material for micro-actuator and for that purpose intrinsic two-way shape memory is desired. An amorphous Ni-Ti film deposited on a substrate of a temperature lower than 573 K is crystallised by holding it at a temperature higher than 673 K and then aged

at a temperature below 773 K in a constrained shape; this aged film shows the two-way shape memory effect [13].

Thin film SMA microdevices can be used to actuate gas membrane microvalves. The main fabrication techniques for these are magnetron sputtering and electrolytic photoetching of the thin films and hybrid integration of the valve components. The SMA microvalves normally work in an open mode and allow control of pressure differences below 2,5 bar at gas flows below 360 cm^3/min [14]. One quite popular and widely used usage of SMAs is as antenna for cellular phones, since superelastic wire is flexible and is not subject to damage. Another example is a medical catheter, which is a tube made of plastics. This tube needs a guide wire, which was previously made of stainless steel but has recently been overtaken by NiTi alloy [10].

2.6 Shape memory alloy composites

Active vibration control can be achieved by incorporating a shape memory alloy in a fiber-reinforced composite as the embedded distributed actuators. NiTi fibers are heat-treated to shape-memorise their initial length at higher temperatures ($<A_f$). They are then quenched to room temperature (to almost martensite start temperature = M_s), subjected to tensile prestrain ε^T (> 0) and embedded in the matrix material to form a composite. The composite is then heated to the temperature ($> A_f$) at which the NiTi fibers shrink back to their initial length by the amount of prestrain ε^T, and then the matrix is subjected to compressive stress. Thus the stress and strain rate of the structure may be modified in a controlled manner[15].

3. Magnetostrictive materials

3.1 Definition

Magnetostriction is observed in a substance when it strains upon application of a magnetic field. Conversely, a field is generated when the material is stressed; this field is, however, proportional to the material's rate of strain. This phenomenon is presented in Figure 3.

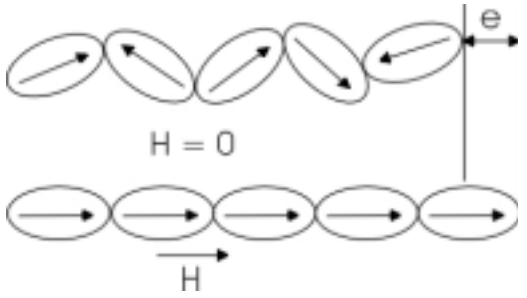

Figure 3. The principle of magnetostriction [44].

3.2 Materials

The modern era of magnetostriction began in 1963 when strains approaching 1% were discovered in the rare earth materials of terbium and dysprosium at cryogenic temperatures. The most frequently used material is giant magnetostrictive Fe-Tb-Dy-alloy called Terfenol-D [1, 44].

3.3 Properties

Magnetostrictive material is usually sold as complete actuator system because the magnetostriction is optimised when the material is both mechanically and magnetically biased. Magnetostrictive material, such as is brittle and the unit must be isolated from side loads or operational moments. Tension should not be increased beyond the rated dynamic force. As with any inductor, the actuator should be protected against any possible damage from a collapsing magnetic field. The commercially-available actuators have total displacement capabilities of 0.2%, are capable of producing output forces of 1750 N, and operate at frequencies up to 60 kHz.

3.4 Applications

Terfenol-D transducers are used as positioners, sonar projectors, isolators, shock absorbing mounts, linear stepper motors, and to mimic the vibrations of an

artificial heart [1]. Linear motors can provide a large stroke of several millimetres and this is limited only by the length available for the translating rod [44, 45].

3.5 Magnetic shape memory materials

Magnetic Shape Memory (MSM) effect is a new invention in the actuator materials field, allowing even 50 times greater strains than in magnetostrictive materials. In MSM materials the magnetic field moves the twins formed in the structure creating a net shape change in the material. The mechanism also enables more complicated shape changes than conventional linear strain, such as bending and shear. Typically, present MSM, such as Ni_2MnGa produce 2% strain at 0 to 2 MPa stress in actuator use. Other potential MSM materials are Fe-Pd and Fe-Ni-Co-Ti alloys [46]. The maximum strain of MSM material is about 5% and the shape change will occur in 0,2 msec. The application temperature range is from –130 to 70 °C [46].

4. Smart polymers

4.1 Nanocomposites and self-assembling polymers

Nanocomposites can be formed in two different ways. One, which uses inorganic nanoscale seeds as a starting point and one, which uses thermodynamically incompatible polymers as a starting point. The applications of these polymers are therefore quite different.

4.1.1 Sol-gel nanocomposites

Sol-gel chemistry produces a variety of inorganic networks from silicon or metal alkoxide monomer precursors. In the early 1970s, monolithic inorganic gels were formed at low temperatures and converted to glasses without a high temperature melting process. Through this process, homogeneous inorganic oxide materials with the desirable properties of hardness, optical transparency,

chemical durability, tailored porosity, and thermal resistance, can be produced at room temperatures.

The technology is based on an innovation, so that precipitation of, for example, SiO_2 or TiO_2 can be controlled with alcohol to produce nanosized particles. The surface of these particles is then modified by, for instance, polymers. The modified particles are melted together to form a composite. Applications include ultrathin coatings to prevent corrosion on steel, magnesium or aluminium. By modifying the surface with fluorosilanes, a non-sticking surface is created [18].

4.1.2 Self-assembling polymers (nanopolymers)

Nanopolymer technology is based on copolymerising three different block polymers. The block polymers are thermodynamically incompatible and they will separate on the nanometer scale (5–100 nm), producing complexly-ordered nanostructures by a process of self-assembly. The assembly of the triblock copolymer can take place, for example, in layers, cylinders or spheres [19].

One goal of the research has been to produce a fuel cell membrane that allows the passage of protons but not the fuel. At least one of the block polymers must be a proton-conductive polymer. Other applications can be nanoscale-reinforced ordered polymer composites or nanoporous materials. Self-assembling polymers work also in thicker sections. Microporous materials could be used for water purification.

4.2 Electroactive polymers (EAP)

Electroactive polymers are polymers that undergo a shape change when a voltage is applied to them. [20]. EAP applications include actuators/switches, motors, sensors and different elastic/shape memory structures. The greatest interest is in developing artificial muscles. The biggest remaining disadvantages are the low force and/or very slow response of the material and the fact that the materials are not robust. Materials that have been tested to induce large displacements include ion exchange membranes, gel polymers, electrostrictives, electrostatics and piezoelectrics [21].

4.2.1 Polypyrrole (PPy)

By applying a voltage over a doped Ppy, it is possible to move the added dopant ions (X^-) and thus impose a change on the volume, conductivity and colour of the doped polymer. By adding a film of doped PPy to a film of gold, a bilayer actuator is formed. Doped PPy also has potential as artificial muscle [22, 23, 24, 25, 26].

The advantage of PPy is that it can be synthesised electrochemically. Several patents have been applied to this technology. Although PPy is inherently conductive, it must be doped to have a usable product. The following figure shows the principle of a micromuscle according to Edwin W. H. Jager et al. [22].

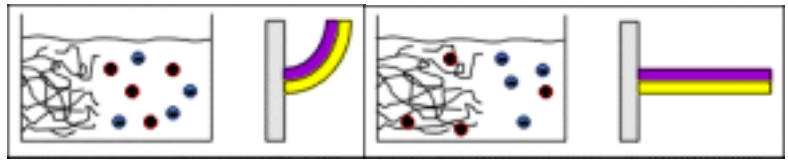

(a) (b)

Figure 4. Oxidised state (a) and reduced state (b).

4.2.2 Fluoropolymers

Muscle actuators, based on double-sided platinum-coated perfluorinated ion-exchange membrane have been constructed. These materials are known also as ionic polymer-metal composites.

4.2.3 Shape memory polymers and polymer gels/foams

Shape memory polymers are another group of shape memory materials. They do not contain metallic compounds and therefore do not exhibit phase changes. They rely on one or more glass transition temperatures to affect a change in state and, unlike their metallic counterparts, shape memory polymers exhibit a reduction in elastic modulus with increasing temperature.

The principle of shape change of a polymer gel is based on thermal cycle (heating-cooling) as in N-isopropylacrylamide hydrogel [31], catalytic reaction as in rutheniumtris (2,2' -bipyridine) /N-isopropylacrylamide hydrogel [30] or magnetic particles (magnetite) containing polyvinyl alcohol (crosslinked with glutaraldehyde) gel [30]. Smart polymer hydrogels show the capability to respond to external stimuli. Smart gels can be tailored to respond to a variety of stimuli such as temperature, pH, light, electric field or magnetic field. However, there is currently only one thermo-reversible gel, poly (N-isopropyl acrylamide) (PNIPAM).

Possible applications are nanosized grippers, drug release gels and artificial heart muscles. Hydrogels can be utilised in novel applications in diverse areas such as sensors, actuators, chemical and biological separation and membranes. The advantage of forming shape memory polymers into foams is that they provide a 3-dimensional shape memory rather than the single axis form commonly found with shape memory alloys. Shape memory foams are commercially available with many different compression characteristics and glass transition temperatures covering dynamic ranges of compression stresses of over 300%. In addition to the advantages of being able to be formed into 3-dimensional shapes, shape memory foams are highly permeable to air thus greatly reducing the time necessary for heating and cooling under forced air conditions [32].

5. Summary

Science and technology are at present relying heavily on the development of new materials. Such materials should be innovative with regard to structure, functionality and design. In this, they will have characteristics similar to those that have been projected for the current generation of smart structures; i.e., embedded sensors, actuators and control mechanisms that are fully integrated to the structure, giving it the ability to sense stimuli imposed upon it and to take an appropriate response to those stimuli in a predetermined and controllable fashion.

However, unlike smart structures, smart materials are fabricated in such a manner that the sensors, actuators and control mechanisms will be part of the microstructure of the material itself. This will typically involve the design, synthesis and processing of such materials at the atomic and/or molecular level.

References

1. Shakeri, C., Noori, M. N. & Hou, Z. Smart materials and structures. http://me.wpi.edu/~cirrus/Publications/SmartMaterials/SmartMaterialExtension.htm

2. Barsoum, R. G. S. Active materials and adaptive structures. Smart Mater. Struct. 1997, 6, pp. 117–122.

3. Steinkopff, T. & Wolff, A. (Siemens AG) Modeling of piezoelectric actuators. Functional Materials, EUROMAT, Wiley, Germany, 2000. Vol. 13, pp. 381–390.

4. Better tennis through piezoelectric fibres? Advanced materials & processes, January 2001.

5. Manz, H. & Schmidt, K. On the application of smart materials in automotive structures, Euromat99, Wiley-VCH Verlag Gmbh, Weinheim, Germany, 2000. Vol. 13, pp. 539–544.

6. Hagood, N. W., Atalla, M. J., Janos, B. Z., Schimidt, M. & Wickramasinghe, V. K. Active fiber composites actuation materials and applications. Euromat99, Wiley-VCH Verlag Gmbh, Weinheim, Germany, 2000. Vol. 13, pp. 496–503.

7. Zhao, C. Shape memory stainless steels. Advanced materials & processes 2001, February.

8. Jang, B. Z. Advanced polymer composites: principles and applications. ASM International, Ohio, USA, 1994.

9. Ju, D.-Y. & Shimamoto, A. Damping property of epoxy matrix composite beams with embedded shape memory fibres. Journal of Intelligent Material Systems and Structures 1999. Vol. 10, pp. 514–520.

10. Otsuka, K. & Ren, X. Recent developments in the research of shape memory alloys. Intermetallics 1999, 7, pp. 511–528.

11. Duerig, T., Pelton, A. & Stöckel, D. An overview of nitinol medical applications. Materials science and engineering 1999. A273-275, pp. 149–160.

12. Van Humbeeck, J. Non-medical applications of shape memory alloys. Materials science and engineering 1999. A273-275, pp. 134–148.

13. Gyobu, A., Kawamura, Y., Saburi, T. & Asai, M. Two-way shape memory effect of sputter-deposited Ti-rich Ti-Ni alloy films. Materials science and engineering 2001. A312, pp. 227–231.

14. Kohl, M., Dittmann, D., Quandt, E. & Winzek, B. Thin film shape memory microvalves with adjustable operation temperature. Sensors and actuators 2000, 83, pp. 214–219.

15. Ju,D.-Y. & Shimamoto, A. Damping property of epoxy matrix composite beams with embedded shape memory fibres. Journal of Intelligent Material Systems and Structures 1999. Vol. 10, pp. 514–520.

16. Porter, G. A., Liaw, P. K., Tiegs, T. N. & Wu, K. H. Fatigue and fracture behavior of nickel-titanium shape-memory alloy reinforced aluminium composites. Materials science and engineering 2001. A314, pp. 186–193.

17. Otsuka, K. & Ren, X. Recent developments in the research of shape memory alloys. Intermetallics 1999, 7, pp. 511–528.

18. Jonschker, G. Nanokomposit – Multifunktionswerkstoffe, Ein neuer Königsweg in der Oberflächenveredelung? Metalloberläche 2000, 12, Jahrg. 54.

19. Brave new nanoworld. ONRL Review. www.ornl.gov/ORNLReview/rev32_3/brave

20. http://ndeaa.jpl.nasa.gov/nasa-nde/lommas/eap/EAP-web.htm

21. Bar-Cohen, Y. Electroactive polymers as artificial muscles – capabilities, potentials and challenges. Robotics 2000 and Space 2000, Albuquerque, NM, USA, 28.2.2000.

22. Jager, Edwin W. H., Smela, Elisabeth & Inganäs, Olle. On-chip microelectrodes for electrochemistry with moveable PPy bilayer actuators as working electrodes. Sensors and Actuators B 1999, 56, pp. 73–78.

23. Okuzaki, Hidenori & Funasaka, Keichi. Electrically driven polypyrrole film actuator working in air. Journal of intelligent material systems and structures 1999. Vol.10, June.

24. Iroh, J. O. & Rajagopalan, R. Electrochemical synthesis of polyaniline-polypyrrole composite coatings on carbon fibres in aqueous toluene sulphonate solution. Surface Engineering 2000. Vol. 16, No. 6, pp. 481–486.

25. In-situ deposited thin films of polypyrrole. http://www.sas.upenn.edu/~macdiarm/

26. Polypyrrole and Polyaniline Doped With Lignosulfonic Acid. http://www.nasatech.com/Briefs/Mar00/KSC11940.htm

27. Bar-Cohen, Y., Xue, T., Joffe, B., Lih, S.-S., Shahinpoor, M., Simpson, J., Smith, J. & Willis, P. Electroactive polymers (EAP) low mass muscle Actuators. SPIE International Conference, Smart Structures and Materials Symposium, San Diego, California, 3–6 March 1997.

28. Shahinpoor, M., Bar-Cohen, Y. Simpson, J. O. & Smith, J. Ionic polymer-metal composites (IPMC) as biomimetic sensors, actuators & artificial muscles – A review. Artificial Muscle Research Institute, University of New Mexico, Albuquerque, New Mexico, USA.

29. Yoshida, Ryo, Yamaguchi, Tomohiko & Kokofuta, Etsuo. Molecular design of self-oscillating polymer gels and their dynamic swelling-deswelling behaviours. Journal of intelligent material systems and structures 1999. Vol. 10, June.

30. Zrinyi, M., Szabo, D. & Kilian, H.-G. Kinetics of the shape change of magnetic field sensitive polymer gels. Polymer Gels and Networks 1998, 6 pp. 441–454.

31. www.calpoly.edu; Smart polymers

32. Monkman, G. J. Advances in shape memory polymer actuation. Mechatronics 2000, 10, pp. 489–498.

33. http://ndeaa.jpl.nasa.gov/nasa-nde/lommas/eap/EAP-web.htm

34. Mather, P. T., Jeon, H. G. & Haddad, T. S. Stain recovery in POSS thermoplastics. Polymer Preprints 2000, 41 (1), pp. 528–529.

35. Matsumoto, Shiro, Sugiyama, Yasuyuki, Sakata, Seizoku & Hayashi, Takayoshi. Light processing and optical devices using nano-sized droplets of liquid crystal dispersed in polymer. Journal of intelligent material systems and structures 1999. Vol.10, June.

36. White-light emitters from smart polymers. Department of Chemistry – University of Otago, New Zealand, Research program, leaders: Brian Robinson and Keith Gordon.
http://neon.otago.ac.nz/chemistry/Research/Materials/whitelight.htm

37. The dawn of Organic electronics. IEEE Spectrum Online, Aug. 2000, Vol. 37, No. 8. http://www.spectrum.ieee.org/publicfeature/aug00/orgs.htm

38. "Smart" fire-resistant polymers under study for use in aircraft. American Chemical Society, 23.3.1999, Anaheim. www.eurekalert.org

39. The Scripps Research Institute; Scientific report 1996–1997. The Skaggs Institute, The Skaggs Institute for Chemical biology.

40. Active Materials Laboratory, MIT, USA. http://aml.seas.ucla.edu/

Manufacturers reports

41. Noliac A/S, Denmark (piezoelectric ceramics)

42. Murata Electronics, USA (piezoelectric ceramics)

43. Shape memory applications, Inc., USA (shape memory alloys, Nitinol)

44. Energen, Inc., USA (magnetostrictive actuators)

45. Etrema Products, Inc. USA (magnetostrictive actuators)

46. AdaptaMat, Finland (MSM actuators)

Application of functional materials based actuators to produce precision motion and force

Tatu Muukkonen & Antero Katainen
VTT Industrial Systems
Espoo, Finland

Abstract

Several different kinds of prototypes were built in the Älytarkkuus project. All the prototypes had actuators based on functional materials. Only those functional materials that were already on the market were chosen. In this project, Shape Memory Alloy (SMA) actuators and Ceramic Multilayer Actuators (CMA) were studied while they were integrated into the innovative constructions designed by VTT. Four prototypes are presented here; one of them is in the patent process. They are all excellent examples of how motion and force can be altered if functional materials are being used.

1. Introduction

Shape Memory as a phenomenon has been known for almost 70 years now, but just recently its availability has clearly increased and the price has come down considerably. Piezoelectric materials have the same trend. New shapes and even better performances keep coming to market, thanks to the development of material technology. Interestingly, producers of the functional materials are very willing to tailor the products to customers' needs. For example, producers have often already trained customers on SMA.

Still, there is a big gap between actuators and industrial solutions. High performance actuators are available, and innovative ideas have already risen among research and development people. The question is how to integrate actuators with construction in a reliable and productive way. Someone should know the background of the functional materials and be able to design,

manufacture, and test at least on a basic level. Such a technical leader could then successfully guide innovative ideas toward industrial solutions. In the Älytarkkuus project, VTT has shown with a few demonstrators how these materials can be utilised in machines and equipment.

2. Prototype Finger

The first prototype is called the Finger for its capability to move like a finger, especially the thumb. The Finger is 350 mm long and has six SMA piston-like actuators. The actuators are integrated into three similar modules innovated and designed by VTT (Fig. 1).

Figure 1. Prototype Finger. The prototype moves like a thumb.

2.1 SMA piston

The SMA piston-like actuator looks like a metallic cylinder. An SMA spring is mounted inside the cylinder. Electric current heats the spring. The length of the spring changes depending on the temperature. In other words, the spring contracts or extends. The maximum change in length (often called the stroke) is 19 mm under a 450 g load. The maximum cycle rate is 1 to 2 times per minute, so the movement is slow. The price is also noteworthy – around 10 € per piece.

2.2 Modules

The Finger has three identical modules made from polypropylene (PP) plastic. The thinnest point in each module is called the joint (or 'solid joint'). These joints were used to avoid a gap between the axle and bearing. The joint is where the module bends 45° (Fig. 2). The joint is designed to bend elastically. Because of the importance of the module's shape, a special method for machining was needed. In this case, Water Jet Cutting was used with success.

Figure 2. Both modules have joints that can bend 45° elastically.

3. Prototype Bridge

The second prototype is called the Bridge. Its span is 300 mm. With this prototype, the change in the shape of its surface could be demonstrated. There are two actuators below the construction, which are both 200 mm long SMA wires with a diameter of 150 µm (Fig. 3). Basically, this type of construction can alter aggressive gas or liquid flow, because the actuators are safely under the surface.

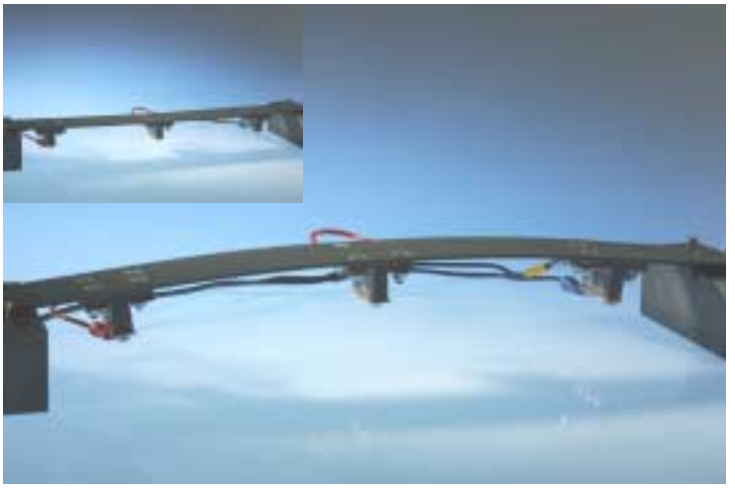

Figure 3. Prototype Bridge changes the shape of its surface.

3.1 SMA wire

Two 20 mm long SMA wires having diameter of 150 µm work as actuators. One wire can hold a load of 330 g and has a maximum stroke of 5% of its length. Both wires hang in the air below the polyvinyl chloride (PVC) bar. Electric current heats the wires; they contract or extend, depending on the temperature. The bar bends 15 mm. The maximum cycle rate of the Bridge is 30 times per minute. This is because the ultra thin wires cool down very rapidly. On the other hand, wires like this are very difficult to bond. The price of this thin, trained wire is about 15 € per meter.

4. Prototype Pat. pend.

The third prototype is in patent pending at the moment. This innovation was done in the area of SMA, even though the phenomena have been known for 70 years.

5. Prototype Gripper

The fourth prototype is called the Gripper (Fig. 4). The prototype is based on a piezoelectric material called Ceramic Multilayer (CMA). This prototype is probably closest to industrial application, because two previous versions have already been made. The very first version was a test stand created to help understand how piezo, strain gauge, and a software program can be connected together. The second version was a real prototype made from a plastic called polyester. It was a study showing how computer-based joint design worked in practise. At the moment, the body of the Gripper is built from aluminium and has a 40 mm-wide opening. It is driven by a computer with a control program. Two strain gauges are used for feedback of movement and force. They sense how much the arms bend during operation. The next version of the Gripper has already been designed and is suitable for industrial use.

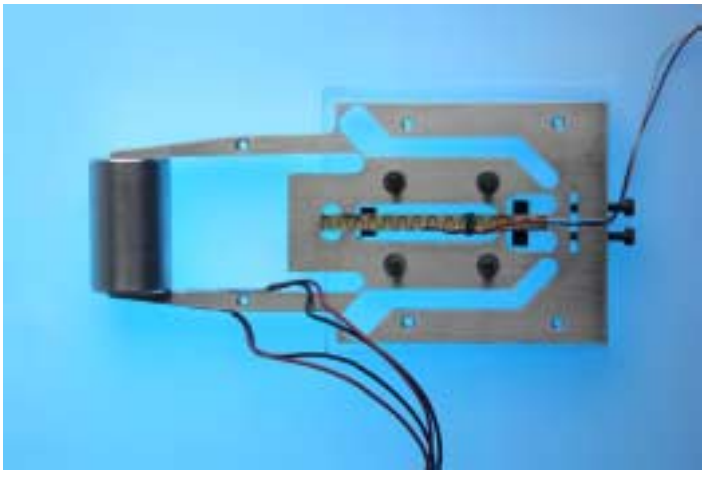

Figure 4. Prototype Gripper is close to industrial application.

5.1 Piezo

The Gripper has one pietzo actuator. The manufacturer calls it Ceramic Multilayer (CMA). The CMA is built up from very thin layers of piezoceramic materials and built-in internal electrodes. The maximum driving voltage is low, 75 V. The maximum stroke of 89 µm is excellent for a piezoceramic material and the maximum force of 1000 N is extremely good. The CMA extends and contracts quickly; the tested cycle rate was 40 Hz. In practise, the maximum rate is probably much faster than that. The CMA actuator is small, with dimensions of 68 x 5 x 5 mm. The price of this actuator is about 500 €.

5.2 Joint design

PRO/Engineer software was used to optimise the construction and joint design. All joints were constructed to bend only elastically. In theory, these joints have no lifetime limitations during normal operation. However, these kinds of joints are very sensitive to overloading.

The Gripper was designed to have three joints on both sides. The joints increase the actuator's stroke by a factor of 80. When the piezo actuator extends 10 µm, the opening between the two arms closes 0,8 mm. Optimised construction was first tested with a plastic model (in this case, polyester). The designed values were attained (Fig. 5).

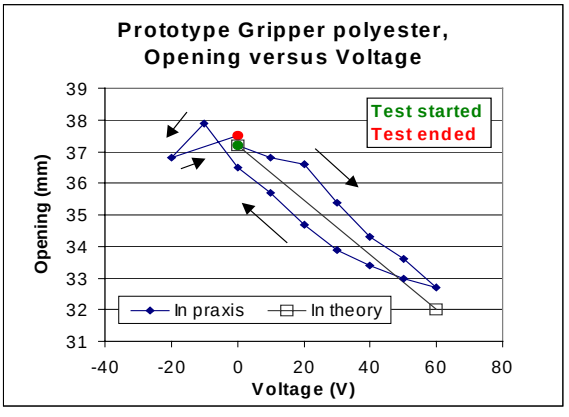

Figure 5. Prototype Gripper polyester, Opening versus Voltage.

In the case of aluminium, FEM modelling was used to analyse and optimise the behaviour of the joints under loading. Movements were magnified and the Gripper's stress distribution was seen during virtual operation. Critical points were easily seen (Fig. 6). Most critical points had stress that exceeded the yield point of the aluminum. The Gripper was then redesigned and machined.

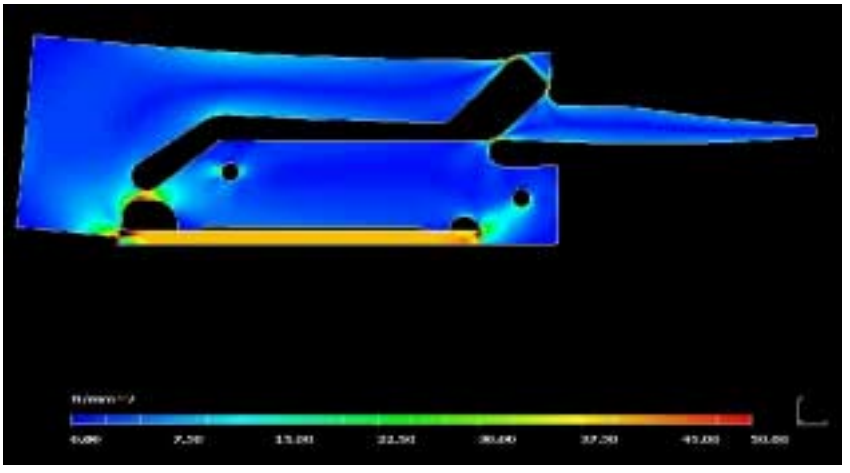

Figure 6. Prototype Gripper aluminum, FEM modelling showed critical points.

5.3 PC control

A real-time operating software program running under MS-DOS controls the Gripper. All essential parameters can be modified. The program reads the set points from the keyboard or a file. This makes the program perfectly suitable for demonstration and test use.

During the operation, the program compares set point values to strain gauge values and optimises the input voltage to the Gripper. The strain gauge values are measured from the left arm bending during the operation. In the future, this signal will be calibrated to show the real force between the arms.

The computer control program was created at Oulu University, Department of Mechanical Engineering.

6. Conclusion

As has been shown in project Älytarkkuus, actuators based on functional materials can be used for controlling precise motion and force. The actuators can be clearly used in place of conventional mechanisms like electric motors and gearboxes. As demonstrated in this project, functional materials and innovative design offer new possibilities for innovation in machine and equipment construction. They enable new functions and reduce the amount of parts in construction. This means that many industrial applications can be replaced by simple, light, and stable actuators that in some cases need only two electrical wires and can be controlled by computer. The real challenge is how to integrate actuators to constructions in a reliable way, that is, to achieve robust design.

Literature

Ball, P. 1998. Mittojen mukaan. 2000-luvun materiaalit. Kimmo Pietiläinen (transl.). Terra Cognita Oy. 562 p. ISBN 952-5202-13-5

Bellouard, Y. 1998. Microgrippers technologies overview. In: IEEE International Conference on Robotics and Automation, Workshop WS4: Precision manipulation at Micro and Nano Scales. Leuven, Belgium, 16–20 May. Pp. 84–109.

Brederholm, A. (ed.) 1995. Funktionaaliset materiaalit ja älykkäät rakenteet koneerakennuksessa. Espoo: Teknillinen korkeakoulu, Konetekniikan osasto, Materiaalitekniikan laboratorio. Julkaisu MTR 1/95.

Janocha, H. 1999. Adaptronics and smart structures: basics, materials, design and applications. Berlin: Springler. 438 p. ISBN 3-540-61484-2

Ullakko, K., Strand, J. & Honkanen, K. 2002. Liikettä tuottavat materiaalit älykkäissä koneissa. Helsinki: Metalliteollisuuden keskusliitto, MET. 54 p. (Teknillinen tiedoitus. MET-julkaisuja 2/2002.) ISBN 951-817-779-1

ER fluids and MR materials – Basic properties and some application developments

Seija Hietanen
VTT Industrial Systems
Espoo, Finland

Abstract

Magnetorheological (MR) and electrorheological (ER) fluids belong to a family of controllable fluids, in which the flow can be controlled through the application of an electric or magnetic field. The rheological properties of controllable fluids typically depend on the concentration and density of particles, particle size and shape distribution, properties of the carrier fluids, additional additives, applied field, temperature and other factors. The interdependency of these factors is very complex, yet it is important in establishing methodologies to optimise the performance of these fluids for particular applications. Unlike ER fluids, MR fluids offer large variations in their rheological properties and their insensitivity to impurities and they require less energy consumption. Recently there has also been interest in creating controllable materials based on elastomers that are loaded with electrically conductive particles. Also a new way of using MR fluids, in which the fluid is contained in an absorbent matrix has been developed. This article gives a short overview of the field of ER fluids and MR materials, their basic properties and some application developments.

1. Introduction

Smart fluid is defined as fluid in which the flow can be controlled through the application of an electric or magnetic field (Sims et al. 1999). Magnetorheological (MR) and electrorheological (ER) materials belong to a family of controllable fluids. Their rheological properties, such as viscosity, elasticity and plasticity, change in the order of milliseconds in response to applied magnetic and electric field levels, respectively (Yalcintas & Dai 1999).

The largest change in the fluid properties occurs when the flow direction is normal in relation to the magnetic field direction (Ashour et al. 1996).

The ability of controllable fluids stems to provide simple, quiet, rapid-response interfaces between electronic controls and mechanical systems makes them interesting. The ability of controllable fluids to be directly used as fast-acting, fluid valves with no moving parts in semi-active vibration control has been one of the principle motivating factors for the development of such fluids (Carlson et al. 1995, Carlson & Sproston 2000).

The field responsive change in rheology exhibited by controllable fluids results from the interaction of polarisable suspended particles. Magnetorheological fluids contain magnetically polarisable particles and so respond to magnetic fields, while electrorheological fluids contain electrically polarisable particles and so respond to electric fields. The interaction between the resulting induced dipoles causes the particles to form columnar structures, parallel to the applied field. These chain-like structures restrict the motion of the fluid, thereby increasing the viscous characteristics of the suspension, see Figure 1. The mechanical energy needed to yield these chain-like structures increases as the applied field increases, resulting in a field-dependent yield stress (Jolly & Nakano 1998).

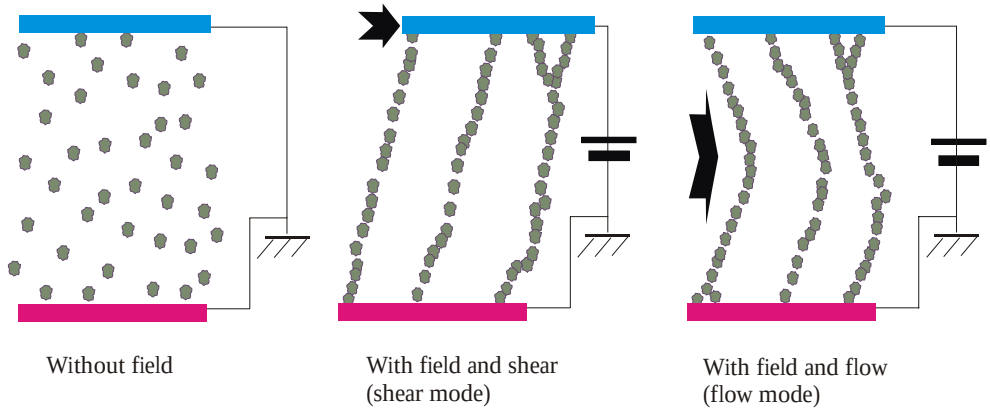

Figure 1. Mechanism of ER effect (within the references of Mäkelä (1999)).

MR elastomers are solid, rubber-like materials whose stiffness may be controlled to provide adjustable mounts and suspension devices. MR foams, in which the controllable fluid is contained in an absorptive matrix, provide a convenient way of realising the benefits of MR fluids in highly cost-sensitive applications (Carlson & Jolly 2000).

This article has been written based on the research report BVAL73-011181 (Hietanen 2001).

2. Development of ER and MR fluids

The ER effect was first discovered by Winslow and the MR effect was discovered by Rabinow in the late 1940s. However, more active research studies on the MR and ER fluids and their applications began in the mid-1980s (Yalcintas & Dai 1999). Research studies of controllable fluids were mostly centred on ER fluids in the mid-1980s and early 1990s (Rankin et al. 1998). Commercially produced ER fluids became available by the mid-1990s (Sims et al. 1999).

Starting in the mid-1990s, research studies were directed at MR fluids and their applications. First MR fluid applications were successfully commercialised in the mid-1990s. Unlike the ER fluids, the MR fluids offer large variations in their rheological properties and insensitivity to impurities, and they require less energy consumption. However the challenges of producing large magnetic fields in a large surface area remain unresolved (Yalcintas & Dai 1999). A chart comparing properties of typical ER and MR fluids is given in Table 1.

Table 1. Comparison of properties of typical ER and MR fluids (Carlson et al. 1995).

Property	ER fluid	MR fluid
Yield strength (Field)	2–5 kPa (3–5 kV/mm) Field limited by breakdown	50–100 kPa (150–250 kA/m) Field limited by saturation
Viscosity (No field)	0.2–0.3 Pas at 25°C	0.2–0.3 Pas at 25°C
Operating temperature	+10–+90°C (ionic, DC) -25–+125°C (non-ionic, AC)	-40–+150°C (Limited by the carrier fluid)
Current density	2–15 mA/cm^2 (4kV/mm, 25°C) (x 10–100 at 90°C)	Can energise with permanent magnets
Specific gravity	1–2.5	3–4
Ancillary materials	Any (conductive surfaces)	Iron/steel
Colour	Any, opaque or transparent	Brown, black, grey/opaque

ER fluids typically exhibit yield strengths within the range of 3 to 5 kPa (Sims et al. 1999). MR fluids are of interest because they typically possess much stronger field-induced interparticle forces, and thus yield stresses, than ER fluids. Apparent yield stresses can reach 100 kPa in flux densities of 1 T or fields of 300 kA/m (Rankin et al. 1998). An MR device can be powered by a low-voltage source (Sims et al. 1999). ER fluids require thousands of volts to operate, while MR fluids operate under much lower voltage, such as a car battery voltage. Hence, safety and packaging are clear design problems for ER fluids (Ashour et al. 1996).

Moreover, the limited temperature operating range of ER fluids has often been cited as a serious constraint to applications in more harsh environments, e.g., in the engine bay of an automobile. Modern ER fluids are usable over temperature range from 15°C to 90°C. MR fluids will operate from -40°C to 150°C, thus increasing significantly the number of potential applications (Sims et al. 1999).

3. Commercial ER and MR fluids

3.1 Structure of ER and MR fluids

Both ER and MR fluids consist of a carrier fluid, particles, surfactants and additives. In order to provide a perfectly suitable fluid for each application, the service purpose and external factors must be thoroughly investigated before designing a new fluid suspension. Features such as the operating temperature, the maximum size and weight of the device, the desired yield stress and requirements due to a static or dynamic situation are crucial design aspects. These requirements will determine the particle size, the maximum volume fraction of particles, stability characteristics, the abrasivity or the need to include surfactants or additives. There is almost no limit to the materials that can be used in an ER or MR suspension, the only difficulty is choosing the right ones for each specific use (Mäkelä 1996b).

The properties of MR (and especially ER fluids) have been recently reviewed by (Mäkelä 1996a–c). MR fluids are considerably less well known than their ER fluid analogues. MR fluid devices have, however, reached commercial applications (Carlson et al. 1995). The remaining part of this article will place its main emphasis on MR fluids and other MR materials.

3.2 Components of MR fluids

In MR fluids the dispersed ferromagnetic carbonyl iron particles are spherical in shape with a diameter size ranging from 1–10 μm. The density of such particles is also high (7–8 g/cm^3). The volumetric concentration of the dispersed particle can be as high as 50% of the total fluid volume (Ashour et al. 1996).

The second component of MR fluid is a carrying fluid, which serves as a continuous insulating medium. Some of the preferred carrying fluids are silicon oils, kerosene, and synthetic oils. The third component of a MR fluid is a stabiliser, which serves to keep the particles suspended in the fluid. There are two kinds of stabilisers: agglomerative stabilisers, which prevent the

ferromagnetic particles from sticking together and sedimental stabilisers, which prevent the particles from settling down with time (Ashour et al. 1996).

Since the number of magnetisable elements and alloys is limited, the choices for MR particulate materials are much more constrained than for ER fluids. However, much greater freedom is possible in selecting suspending fluids and additives, since the dielectric properties of the suspending fluid do not influence the MR effect (Rankin et al. 1998). Because the magnetic polarisation mechanism is not affected by the surface chemistry of surfactants and additives, it is relatively easy to stabilise MR fluids against particle-liquid separation in spite of the large density mismatch (Carlson & Jolly 2000). For high-strength MR fluids carbonyl iron is a typical choice as it possesses a large saturation magnetisation, it is relatively inexpensive and available in large quantities (Rankin et al. 1998).

4. Properties and characterisation

4.1 Rheological properties

The rheological properties of controllable fluids typically depend on the concentration and density of particles, particle size and shape distribution, properties of the carrier fluids, additional additives, applied field, temperature and other factors. The interdependency of these factors is very complex, yet it is important in establishing methodologies to optimise the performance of these fluids for particular applications (Jolly et al. 1999). One of the critical obstacles to progress in developing ER and MR fluids has been a lack of understanding in the underlying mechanisms of electro- and magnetorheology (Rankin et al. 1998). Because of the nature of the controllable fluids, it seems likely that the experimental technique will continue to play a significant role in the modelling of controllable fluids (Sims et al. 1999).

The field responsive effect of the commercial fluids is shown in Figure 2. At low fields, both MR and ER fluids are seen to exhibit a sub-quadratic relationship between stress and field. This sub-quadratic character is attributed to gradual particle saturation in MR fluids. Beyond fields of about 0.1 Tesla, the stress response begins to plateau as the MR fluid approaches complete magnetic

saturation (Jolly & Nakano 1998). The flux density at which magnetic saturation occurs increases as the iron volume fraction in the fluid increases (Jolly et al. 1999). ER fluids, on the other hand, exhibit dielectric breakdown long before fields are achieved at which saturation mechanism arise. Because of dielectric breakdown, the stress levels that ER fluid can achieve are typically one to two orders of magnitude less than the stresses achieved by MR fluids. Figure 3 shows the viscosity of the controllable fluids as a function of shear rate. ER fluids are typically less viscous than MR fluids in the range 10^2–10^3 1/s (Jolly & Nakano 1998).

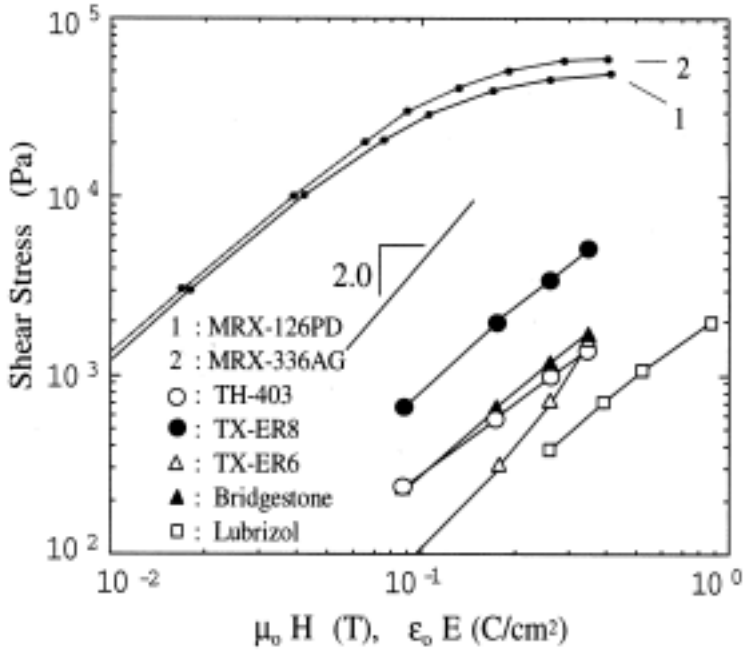

Figure 2. The field-dependent rheological effect of commercial ER and MR fluids. The MR fluid data was measured at 30/s and the ER fluid data at 200/s. Symbols: μ_0 is permeability of vacuum, H is field in MR fluid, ε_0 is permittivity of free space and E is field for ER fluid (Jolly & Nakano 1998).

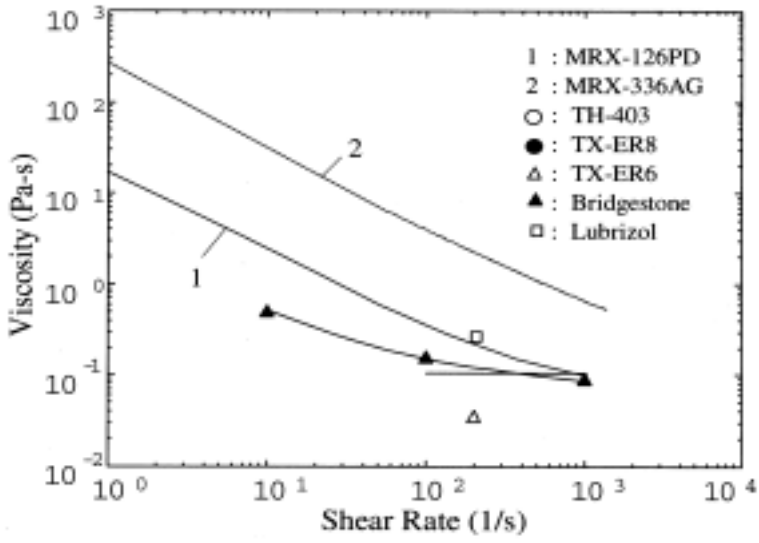

Figure 3. Viscosity as a function of shear rate at zero field (Jolly & Nakano 1998).

In any MR fluid characterisation study, the following minimum data are required. The initial viscosity of the fluid at zero shear rate, shear stress versus shear strain rate data over a range of applied magnetic field strengths, yield stress values at different yield strengths, temperature dependence of the shear stress and qualitative long term stability behaviour. A "good" MR fluid is characterised by a low initial viscosity, high shear stress values at a certain field strength, negligible temperature dependence, and high stability (Ashour et al. 1996). In MR fluids the viscosity in the absence of field is most significantly a function of the carrier oil, suspension agents and particles (Jolly et al. 1999).

Most devices that use controllable fluids can be classified as having either fixed poles (pressure-driven flow mode) or relatively sliding poles (direct shear mode). Examples of pressure-driven flow mode devices include valves, dampers and shock absorbers. Examples of direct shear mode devices include clutches, brakes and locking devices. A third mode, squeeze-film mode, has also been used in low motion, high force applications (Jolly & Nakano 1998). Diagrams of these two basic operational modes are shown in Figure 4.

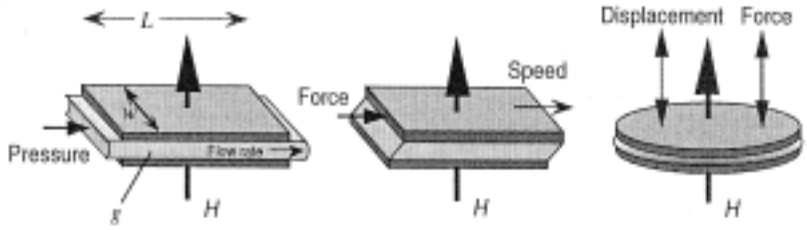

Figure 4. Basic operational modes for controlling ER and MR fluid devices: (a) pressure-driven mode, (b) direct shear mode and (c) squeeze mode (Carlson 1999).

4.2 Lubricity, settling characteristics, and material compatibility

Inherently MR fluid is somewhat abrasive. The degree to which it will affect the durability of a particular part or component depends on a number of factors associated with fluid composition and device design. Materials that are exposed to MR fluid in direct sliding contact are often critical abrasion regions, particularly in linear device applications. The ability of MR fluids to lubricate sliding surfaces will reflect the propensity for wear of such surfaces within MR fluid-based devices (Jolly et al. 1999).

As with any micron-scale particulate suspension in which a density mismatch between the particulate and surrounding fluid exists, settling in MR fluid must be considered when formulating. The specific application dictates to what extent settling must be controlled and how it is to be measured (Jolly et al. 1999).

Other criteria governing the composition of an MR fluid include the device operating temperature range, compatibility with materials within the device, and whether or not the fluid will be sealed from the atmosphere (Jolly et al. 1999).

5. Applications and MR fluid products

5.1 MR fluid rotary brake

In 1995 a mass-produced MR fluid rotary brake was introduced onto the exercise equipment market as a variable resistance element for use in microprocessor-controlled aerobic stair climbers and cyclical machines (Carlson & Sproston 2000).

5.2 Semi-active MR dampers for seats

In 1998 a real-time, semi-active vibration control system became available for usage in the seats of trucks (Carlson & Sproston 2000). The MR fluid damper shown in Figure 5 is a small, monotube damper designed for usage in a semi-active seat suspension system on large on- and off-highway vehicles. The MR damper is capable of providing a wide dynamic range of force control for very modest input power levels, as is shown in Figure 6. The MR fluid valve and associated magnetic circuit are fully contained within the piston. An input power of 5 watts is required to operate the damper at its nominal design current of 1 A (Jolly et al. 1999).

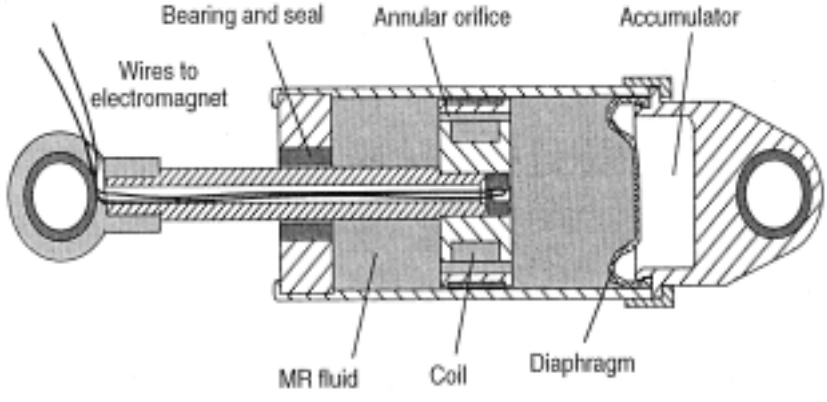

Figure 5. MR fluid damper for seat suspension (Carlson 1999).

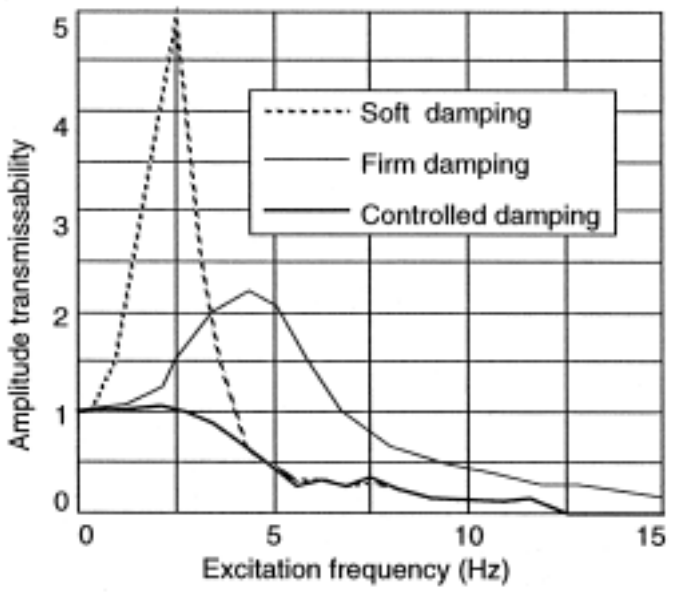

Figure 6. Performance of a MR semi-active controlled suspended seat (Carlson 1999).

5.3 MR fluid shock absorbers for cars

In 1998 MR fluid-based, adjustable shock absorbers for racing automobiles were introduced by Carrera (MagneShock). A set of four of these controllable MR fluid dampers may eliminate the necessity of maintaining the usual stable of dozens of different passive hydraulic shock absorbers. Car operators no longer need to physically change shock absorbers to optimise their vehicles to the conditions of track, weather or tire condition (Carlson & Sproston 2000). Delphi has announced that their version will be available on some 2003 Cadillac models (http://www.carrerashocks.com/MagneShock.htm, http://www. delphiauto.com).

5.4 Steer-by-wire

An MR rotary brake is used to provide real-time sensor feedback to the operator of an industrial forklift vehicle that is operated by a steer-by-wire system. There is no mechanical connection between the steering wheel and the ground wheels.

It is suitable to close maneuvering in clean-spaces such as food handling warehouses with large drive-in freezers. Steering is accomplished by electrical control (Carlson & Sproston 2000).

5.5 Industrial pneumatics

MR fluid rotary brakes and linear dampers are used in conjunction with pneumatic actuators to enable open- and closed-loop position and velocity control with precision not normally achievable with pneumatic systems (Carlson & Sproston 2000, http://www.mrfluid.com).

5.6 Advanced prosthetics

A small MR fluid damper is used to control, in real-time, the motion of a prosthetic knee (Carlson & Sproston 2000). The prosthesis, which uses an MR fluid damper, enables above-the-knee amputees to walk with a more natural gait and makes climbing up and down stairs and inclines much easier than before. Response time is milliseconds (http://www.mrfluid.com/prosthetic_ applications.htm).

5.7 Seismic motion control

Civil engineers in the construction industry are presently incorporating MR damping technology into the structural engineering of buildings and bridges. The system is relatively inexpensive, needs little maintenance and requires very little power to operate. The damping system works similarly to an automotive shock absorber, protecting the structure from earthquakes and windstorms. Stay cables are prone to vibration due to wind and rain. Smart dampers have a potential efficiency several times that of standard oil dampers (http://www.mrfluid.com/seismic_mitigation.htm).

6. MR elastomers

6.1 Background for MR elastomers

With increasing attention being given to the noise, vibration and harshness characteristics of vehicle power trains and chassis system, the limitations of the conventional elastomers have become more problematic. For example, their stiffness and damping cannot always be adjusted independently or optimised for all operating conditions and even variable orifices or electric actuators for enabling active control of components characteristics have been developed (Ginder et al. 1999).

During the 1990s, there was an interest in creating controllable materials, based on elastomers that are loaded with electrically conductive particles. Such elastomers could become a link, bringing the applications of modern control technologies, intelligent structures, and smart materials to a very broad industrial area (Jolly et al. 1996).

6.2 Properties of MR elastomers

Carbonyl iron or other magnetisable particles are added to the polymer-material prior to crosslinking. Prior to and during crosslinking, a strong external magnetic or electrical field is applied to the composite. This field induces a dipole moment within each particle. The particles respond by attempting to migrate to minimum energy states, which in this case are particle chains with collinear dipole moments parallel to the applied field. As the elastomer composite cures, the crosslinking process – during which polymer molecules interconnect – locks the imbedded particle chains in place. The shearing of cured composite in the presence of a magnetic field causes particles displacement from a minimum energy state thereby requiring additional work. In principle, this required additional work rises monotonically with the applied field, thus resulting in a field dependent shear modulus (Jolly et al. 1996, Ginder et al. 1999).

For elastomer composites containing magnetically soft particles dispersed in natural rubber, a 30% to 40% maximum change in modulus was observed upon

the application of a saturating magnetic field (Ginder et al. 1999). The field-induced modulus increase is substantial even at kilohertz mechanical frequencies (Ginder et al. 2001). These substantial modulus changes make the use of these composites in variable stiffness devices feasible. While the field-induced change in modulus was found to be nearly entirely dependent upon the particle volume fraction, arrangement and magnetic properties, further improvements in controllability can be accomplished by reducing the nominal modulus of the composite. This observation advocates the incorporation of magnetically permeable particles into softer matrices such as foams (Jolly et al. 1996).

It has been observed that elastomer composite materials are anisotropic in terms of mechanical, magnetic, electrical and thermal properties (Jolly et al. 1996). Large, positive magnetostrictive length change, induced by an uniform applied field, was also observed (Ginder et al. 2001).

6.3 Applications of MR elastomers

This technology may be broadly applicable to various vibration isolation and motion control problems encountered on vehicles and during manufacturing (Ginder et al. 1999). Elastomers with field responsive rheology hold the promise of enabling simple variable stiffness devices. In literature there are countless applications for systems that employ a variable stiffness, such as adaptive tuned vibration absorbers, stiffness tunable mounts and suspensions and variable impedance surfaces. Ford Motor Company has patented an automotive bushing employing a MR elastomer (Ginder et al. 1999, Carlson & Jolly 2000).

7. MR foams

7.1 MR fluid sponge devices

A MR sponge device contains MR fluid that is constrained by capillary action in an absorbent matrix such as sponge, open-celled foam, felt or fabric. The absorbent matrix serves to keep the MR fluid located in the active region of the device where the magnetic field is applied. The absorbent matrix allows a minimum volume of MR fluid to be operated in a direct shear mode without

seals, bearings or precision mechanical tolerances. The absorbent matrix is normally attached to one of the poles, which may move relative to the other pole. Application of the magnetic field causes the MR fluid in the matrix to develop a yield strength and resist shear motion. This basic arrangement may be applied in both linear and rotary devices wherever the direct shear mode would normally be used (Carlson 1998).

8. Summary

Magnetorheological (MR) and electrorheological (ER) fluids belong to a family of controllable fluids, in which the flow can be controlled through the application of an electric or magnetic field. Controllable fluids stems are interesting because of their ability to provide simple, quiet, rapid-response interfaces between electronic controls and mechanical systems. The ability of controllable fluids to be directly used as fast-acting, fluid valves with no moving parts in semi-active vibration control has been one of the principle motivating factors for the development of such fluids.

The rheological properties of controllable fluids typically depend on concentration and density of particles, particle size and shape distribution, properties of the carrier fluids, additional additives, applied field, temperature, and other factors. The interdependency of these factors is very complex, yet it is important in establishing methodologies to optimise the performance of these fluids for particular applications. Because of the nature of the controllable fluids, it seems likely that the experimental technique will continue to play a significant role in the modelling of the controllable fluids.

The first MR fluid applications were successfully commercialised in the mid-1990s. Unlike the ER fluids, MR fluids offer large variations in their rheological properties and insensitivity to impurities, and they require less energy consumption. MR fluids offer a dramatic improvement over ER fluids in the magnitude of the storage modulus. Thus MR fluids are capable of performing better than ER fluids in damping applications that require the controllability of stiffness.

During 1990s there has been interest in creating controllable materials based on elastomers that are loaded with electrically conductive particles. Such elastomers could become a link, bringing the applications of modern control technologies, intelligent structures, and smart materials to a very broad industrial area.

Recently, a new way of using MR fluids, in which the fluid is contained in an absorbent matrix, has been developed. Such MR sponge devices enable the benefits of controllable MR fluids to be realised in cost-sensitive applications. Low-cost, controllable MR sponge dampers are particularly appropriate for moderate-force vibration control problems where a high degree of control is desired.

MR elastomers and MR foams are still at development stage and number of applications is still limited. Research is still needed in order to fully utilise the extraordinary properties of controllable fluids, MR elastomers and MR foams.

References

Ashour, O., Rogers, C. A. & Kordonsky, W. 1996. Magnetorheological fluids: materials, characterization, and devices. Journal of Intelligent Material Systems and Structures, Vol. 7, pp. 123–130.

Carlson, J. D., Catanzarite, D. N. & St. Clair, K. A. 1995. Commercial magneto-rheological fluid devices. In: Bullough, W. (ed.). Proceedings of 5th International Conference on ER Fluids, MR Suspensions and Associated Technology, Sheffield 10–14 July 1995. World Scientific. Pp. 1–9.

Carlson, J. D. 1998. Low-cost MR fluid devices. In: Borgmann, H. (ed.). Actuator 1998. 6th International Conference on New Actuators, Bremen 17–19 June 1998. Bremen: Messe Bremen GMBH. Pp. 417–421. ISBN-3-933339-00-6

Carlson, J. D. 1999. Magnetorheological fluid actuators. In: Janocha, H. (ed.). Adaptronics and smart structures: basics, materials, design, and applications. Heidelberg: Springer-Verlag. Pp. 180–231. ISBN 3-540-61484-2

Carlson, J. D. & Jolly, M. R. 2000. MR fluid, elastomer and foam devices. Mechatronics, Vol. 10, pp. 555–569.

Carlson, J. D. & Spronston, J. L. 2000. Controllable fluids in 2000 – status of ER and MR fluid technology. In: Borgmann, H. (ed.). Actuator 2000. 7th International Conference on New Actuators and Drive Systems, Bremen 19–21 June 2000. Bremen: Messe Bremen GMBH. Pp. 126–130. ISBN-3-933339-02-2

Ginder, J. M., Clark, S. M., Schlotter, W. F. & Nichols, M. E. 2001. Magnetostrictive phenomena in magnetorheological elastomers. In: Bossis, G. (ed.). 8th International Conference on ER Fluids and MR Suspensions, Nice July 9–13, 2001. To be published. 7 p.

Ginder, J. M., Nichols, M. E., Elie, L. D. & Tardiff, J. L. 1999. Magnetorheological elastomers: properties and applications. In: Proceedings of the SPIE – The International Society for Optical Engineering. Smart Materials Technologies, Vol. 3675. Newport Beach, California, March 1999. SPIE-Int. Soc. Opt. Eng.. Pp. 131–138.

Hietanen, S. 2001. ER fluids and MR materials – Basic properties and some application developments. Espoo: Technical Research Centre of Finland (VTT). Research report BVAL73-011181. 27 p.

http://www.carrerashocks.com/MagneShock.htm Web pages for Carrera, Atlanta, GA, USA.

http://www.delphiauto.com Web pages for Delphi Automotive Systems, Troy, Michigan, USA.

http://www.mrfluid.com Web pages for Lord Corporation, Cary, NC, USA.

Jolly, M. R., Bender, J. W. & Carlson, J. D. 1999. Properties and applications of commercial magnetoreological fluids. Journal of Intelligent Material System and Structures, Vol. 10, pp. 5–13.

Jolly, M. R., Carlson, J. D., Munõz, B. C & Bullions, T. A. 1996. The magnetoviscoelastic response of elastomer composites consisting of ferrous particles embedded in a polymer matrix. Journal of Intelligent Material Systems and Structures, Vol. 7, pp. 613–622.

Jolly, M. R. & Nakano, M. 1998. Properties and applications of commercial controllable fluids. In: Borgmann, H. (ed.). Actuator 1998. 6th International Conference on New Actuators, Bremen 17–19 June 1998. Bremen: Messe Bremen GMBH. Pp. 411–416. ISBN-3-933339-00-6

Mäkelä, K. K. 1996a. Electro- and magnetorheological fluids. Part 1. Fundamentals. Tribologia, The Finnish Journal of Tribology, Vol. 15, No. 1, pp. 41–47.

Mäkelä, K. K. 1996b. Electro- and magnetorheological fluids. Part 2. Material aspects. Tribologia, The Finnish Journal of Tribology, Vol. 15, No. 2, pp. 3–15.

Mäkelä, K. K. 1996c. Electro- and magnetorheological fluids. Part 3. Applications. Tribologia, The Finnish Journal of Tribology, Vol. 15, No. 3, pp. 35–51.

Mäkelä, K. K. 1999. Characterization and performance of electrorheological fluids based on pine oils. Espoo: Technical Research Centre of Finland (VTT). 69 p. (VTT Publications 385). ISBN 951-38-5373-X

Rankin, P. J., Ginder, J. M. & Klingenberg, D. J. 1998. Electro- and magneto-rheology. Current Opinion in Colloid & Interface Science, Vol. 3, No. 4, pp. 373–381.

Sims, N. D., Stanway, R. & Johnson, A. R. 1999. Vibration control using smart fluids: a state-of-the-art review. The Shock and Vibration Digest, Vol. 31, No. 3, pp. 195–203.

Yalcintas, M. & Dai, H. 1999. Magnetorheological and electrorheological materials in adaptive structures and their performance comparison. Smart Materials and Structures, Vol. 8, pp. 560–573.

MR fluid-based damping force control for vehicle cabin vibration suppression

Ismo Vessonen
VTT Industrial Systems
Espoo, Finland

Abstract

The goals of the research contribution presented in this paper were to gather knowledge on the dynamic properties of adjustable magnetorheological fluid (MR fluid) dampers, to test and compare semi-active skyhook and fuzzy control algorithms and to gain expertise in the practical application of MR dampers and semi-active control methods.

The research work included dynamic loading tests of a single MR damper to characterise dynamic damper force behaviour, plus computer simulations to design and compare different control system approaches. In the final phase, laboratory test bench measurements for a tractor cabin assembly equipped with MR dampers and a control system were conducted to test alternative control schemes and the complete system.

The main conclusion is that the MR fluid-based semi-active vibration control system is a feasible new technique. It includes promising features for various suspension needs in mobile machines, for which better performing and cost-effective alternatives for rigid joints and passive suspension are required.

1. Introduction

Throughout the international vehicle industry there is a growing interest in novel and advanced suspension structure that can improve the driving comfort and handling properties of the end products. In traditional passive suspension systems, the requirements for driving comfort on the one hand and handling on the other are always at odds and compromises have to be made. Moreover, and

most especially in mobile machines, there is demand for additional suspension features such as adjustable ground clearance and vehicle body attitude control.

Both semi-active and fully-active suspension systems provide possibilities to tune and adjust, in continuous real-time operational mode or by using predefined states of operation and suspension properties for varying operational conditions (vehicle loading, road conditions, road roughness, temperature etc.). Having this kind of flexibility in usage, it is possible to implement, by the careful application of design practice, optimised suspension solutions in respect to both comfort and handling characteristics.

The main difference between semi- and fully-active systems is that fully-active systems need a continuous external energy supply to maintain the control forces. Semi-active implementations modify the stiffness and the damping characteristics of the suspension without the need to supply a substantial amount of external energy. Only a small quantity of energy is needed to perform the control operations. It is a combination of the relatively simple and inexpensive structure, the low operational power requirement and the possibility to achieve good motion and vibration suppression performance that make the semi-active suspensions very attractive alternatives to fully active solutions for practical vehicle applications.

Usually only the damping properties of the suspension assembly are adjusted in semi-active implementations. One possibility of achieving controllable damping force would be to develop existing passive hydropneumatic dampers by adding variable orifice hydraulic flow control valves. Another alternative would be to apply magneto (MR) or electrorhelogical (ER) fluids, with which the fluid flow is controlled through the application of a magnetic or electric field affecting the rheological properties of the fluid. For practical applications, MR fluids offer several advantages over ER fluids. Therefore a MR fluid-based damping control system is an alternative of great potential for the implementation of commercial semi-active suspension systems.

This article is based on the research work done in the "Active Vibration Control" (AVC) subproject of the VTT Industrial Systems´ internal technology program "Smart materials and structures" (ÄLYMARA) extending from the years 2000–2002.

The goals of the semi-active control task within the AVC- subproject were the following:

- To gather knowledge on the dynamic properties and behaviour of MR fluid dampers
- To test and compare semi-active skyhook and fuzzy control algorithms
- To gain know-how on applying MR dampers and semi-active control methods to a practical case, which was selected to be a laboratory test bench with a full-scale agricultural tractor cabin installed on the bench.

2. MR fluids and their pros and cons

Magnetorheological fluid (MR fluid) is a functional material consisting of carrier liquid, ferro-magnetic particles, plus some additives, which are included to work against particle-liquid separation and wear of sealings, for example. When an external magnetic field is applied to the fluid, the magnetic particles form chain-like structures, parallel to the field. The result of this is that the yield strength of fluid is increased in proportion to the applied magnetic field. A MR fluid-based damper can be constructed by arranging the fluid so that it flows through a narrow orifice, across which the controllable magnetic field, induced by a proper coil assembly, is applied. Figure 1 illustrates the operation principle of a MR fluid working in flow control mode.

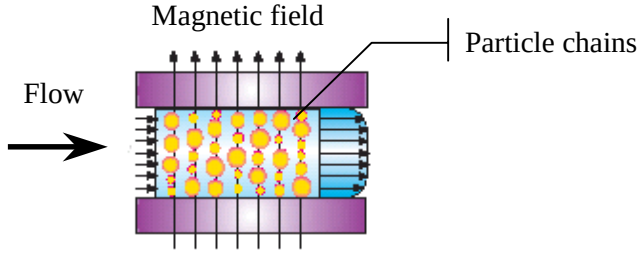

Figure 1. MR fluid working in flow control mode.

The pros and cons of MR fluid-based adjustable damping devices are summarised in Table 1.

MR dampers are relatively simple devices and are to a large extent analogous to the ordinary passive sock absorbers so common in different vehicles. One important feature of these dampers is the fast response time, which is especially useful in continuous real-time damping force control. The low control power requirement is also a valuable feature, when considering the energy efficiency of suspension control.

The best known disadvantage of MR fluids is the particle-liquid separation, which is due to gravitation settling when the MR device remains static for a long time period. However, this settling is to a large extent avoidable with the proper selection of the carrier liquid, surfactants and additives. Yet at the same time, the most important avoidable feature is the agglomeration, i.e., particles sticking permanently together so that they will not mix with the carrier liquid when the fluid is moved again. If the fluid is properly designed, the mixing of the particles takes place within a few operation cycles of the device, and the original characteristics are thus rapidly restored.

Table 1. Pros and cons of MR fluid based damping devices.

+	Simple and robust interface between electronic control and mechanical damping force
+	Fast response (< 10 ms), high damping force bandwidth
+	Powering from common low-voltage sources (DC 12–24 V), power consumption (max. 50 W)
+	Insensitivity to temperature and contaminants, typical temperature range -40…+150 ºC
+	Scaleable also to high damping force applications
-	Particle/carrier oil separation can take place (controllable)
-	Wear of seals (controllable)
-	Price of the fluid at the moment (500–1000 $/l, small amount)

3. Semi-active control algorithms

3.1 Skyhook damping scheme

One of the best known semi-active control scheme is the skyhook control law introduced by professor Karnopp et al. (Karnopp et al. 1974). The basic principle of skyhook control is illustrated in Figure 2 with a simple 1 degree-of freedom (1-dof) system, where the vibration excitation comes through the base excitation (as is the case in tractor cabin vibration). The aim is to efficiently isolate the mass from the base excitation, and at the same time, to avoid unnecessary large relative motion between the base and the mass. The idea behind skyhook control is to utilise a simple damper to reduce the absolute vibration velocity of the suspended mass (Figure 2, damper b). In this way it is possible to achieve a better combination of resonance frequency range damping and high frequency band damping than in the case of a passive damping device between the base and the mass to be isolated.

It is quite evident that the basic idea is not very practical, because it assumes that a firm attachment point in space, i.e., a "skyhook", should exists. This point should then follow the moving mass so as to be able to produce damping force relative to the absolute velocity of the mass. In practice, the best way to simulate the skyhook damper is to put an adjustable damper between the base and the suspended mass, and to try to mimic the behaviour of the skyhook device. In this way the adjustable device produces damping force relative to the relative velocity between the base and the mass (Figure 2 damper c).

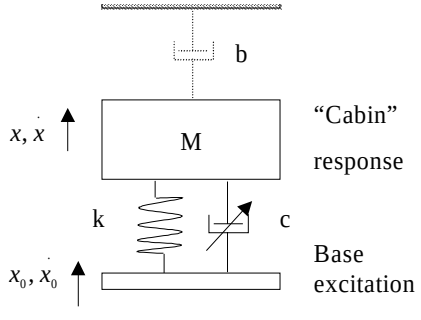

Figure 2. The principle of the skyhook damping system.

The skyhook control law for this more practical case is stated in Equations 1a and 1b (Karnopp et al. 1974).

$$F_d = b * \dot{x}, \quad \text{if} \quad \dot{x}(\dot{x} - \dot{x}_0) > 0 \qquad (1a)$$

$$F_d = 0, \quad \text{if} \quad \dot{x}(\dot{x} - \dot{x}_0) < 0 \qquad (1b)$$

The desired force level F_d is the damping coefficient b times the absolute velocity of the mass if the product of the absolute velocity of the mass and the relative velocity between the mass and the base structure are greater than zero (Equation 1a). If this product is lower than zero, the control law would require the damper to supply power to the system, which it cannot do due to the purely dissipative nature of the device. In this case, the best that can be done is to set the damping force to zero (Equation. 1b).

A simulation model of the simple 1-dof system in Figure 2 with the ideal skyhook damping system was set up using MATLAB/Simulink program. In this context "ideal" means that the adjustable damper device is capable of producing any desired damping force from zero to infinity without any delays in operation. In Figure 3 there are time history plots from simulation where the base velocity excitation amplitude is 0,4 m/s at sinusoidal frequency 2,5 Hz. Other parameters of simulation are: mass is 400 kg, spring stiffness 28000 N/m and desired damping coefficient b_{crit} is 6700 Ns/m. These parameters represent the relevant values for the tractor cabin vibration control case.

How the required damper force goes to zero, when the skyhook criterion (Equation 1a–b) is lower than zero can be seen from the upper plot. Also noteworthy are the abrupt changes in the force amplitudes during a single cycle of vibration.

In Figure 4 there is a simulated (1-dof system with the above indicated parameters, here the mass is referred as "cabin") third octave acceleration spectra for skyhook control with more random base excitation, measured on a real agricultural tractor driving on a ploughed field. Here the dashed line represents the base excitation and the solid lines are the "cabin" acceleration spectra for various desired skyhook damping levels. The widest solid line is for the required

damping level of 50% of the critical and shows rather good vibration suppression performance within the main excitation frequency range of 2–4 Hz.

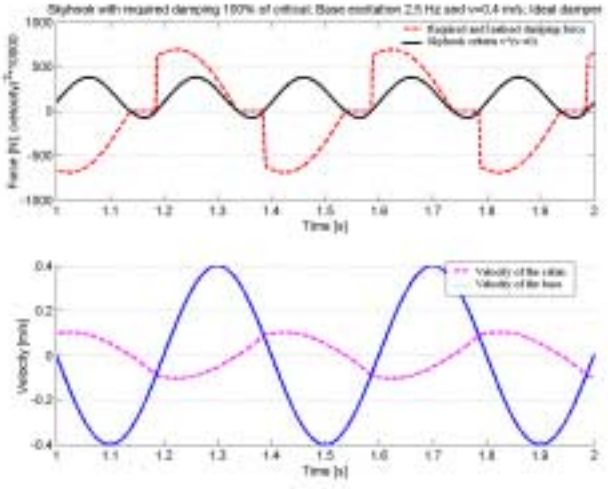

Figure 3. Upper plot: Skyhook criterion (solid line) and required damping force (dashed line). Lower plot: Base velocity (solid line) and velocity of the isolated mass (dashed line). Base excitation 0,4 m/s at 2,5 Hz.

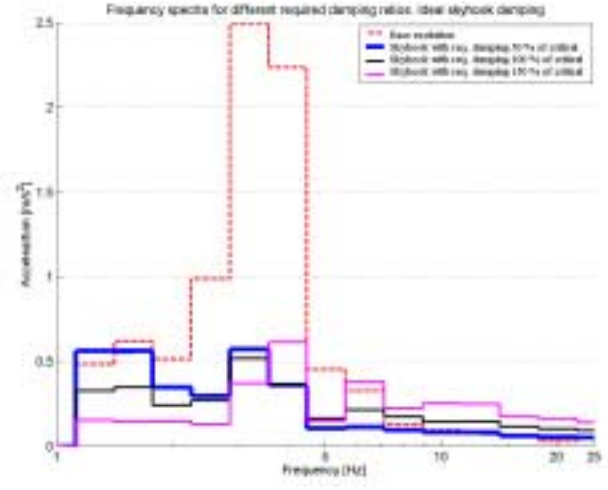

Figure 4. Third octave acceleration spectra for base excitation (dashed line) and for "cabin" acceleration with various levels of required damping (solid lines).

4. Fuzzy control scheme

Fuzzy logic, developed in the mid 60´s, has since 70´s steadily found new applications in the implementation of expert systems and control algorithms.

The basic structure of a fuzzy control process is shown in Figure 5 (Vähänikkilä, 2001). The exact measurements used as control inputs are fuzzified, i.e., transferred into linguistic form using so-called membership functions. This is done in order to be able to use these inputs in fuzzy reasoning by using the rules table, which is the core of the control system. The result of the reasoning phase using fuzzy logical operations is a fuzzy subset, which can be illustrated as a certain subarea in the output signal membership function plot. From the practical point of view, only one single output value per output variable can be used in process control, and thus the output "area" should be defuzzified to give this single control output value. This is usually done with the so-called centre-of-gravity principle.

The fuzzy control experiments in the tractor cabin test bench were conducted in collaboration with the Machine Design Laboratory of the University of Oulu. One researcher designed several fuzzy controller versions for tractor cabin tests using the FuzzyTech design program, from which the C-language code for the actual controller could be output directly so as to be incorporated into the control code of the test bench. The absolute velocity of the cabin and the relative velocity between the bench and the cabin, both integrated from measured accelerations, were mainly used as input signals of the fuzzy controller. The output signal was the control voltage to the electronic control box of the MR dampers. The same control voltage was applied to both dampers at the two rear corners of the tractor cabin.

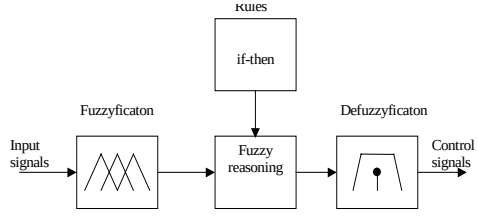

Figure 5. The basic structure of fuzzy control process.

One example of an applied rules table is illustrated in Figure 6, where the measured data on the MR damper force characteristics and the skyhook principle are utilised to establish rules for various input signal combinations.

		Cabin velocity		
		Negative	*Zero*	*Positive*
Suspension velocity	*Negative*	ME	VL	VL
	Zero	VL	VL	VL
	Positive	VL	VL	ME

where the linguistic values are: ME = Medium , VL = Very Low

Figure 6. An example of the rules table of a fuzzy controller for semi-active damping control.

5. Experiments in the tractor cabin test bench

Figure 7 illustrates the test arrangement for the semi-active control experiment using MR dampers. The dampers are positioned at the two rear corners of the cabin and are intended to suppress the vertical vibration of the cabin. At the forward corners of the cabin, a stiff air spring and a hydraulic damper with a high damping ratio support the structure. A plastic barrel is tied on the cabin seat, supported by an air spring and a damper, to simulate the weight of the driver.

An existing hydraulic test bench, owned by VTT Electronics in Oulu, was used in the experiment. With this test arrangement it was possible to separately control the transverse rolling and longitudinal pitching motion of the cabin by regulating the motion of the hydraulic actuators of the bench. The velocity signals measured on the real tractor while driving on a ploughed field were input so as to control the motion of these hydraulic excitation actuators.

To calculate the semi-active control inputs, two accelerometers were used to measure the motion state of the system: One at the rear part of the cabin and the other at a corresponding position on the bench side. The control algorithms were first tuned on the basis of these measurements, but later several accelerometers

positioned all over the test structure were used in the final vibration suppression performance tests of the system.

Figure 7. Tractor cabin test bench (left) and the two MR damper/coil spring sets installed between the cabin and the bench. The hydraulic hoses and the associated block are not part of this experiment.

The MR dampers used in the experiments are commercially available components, originally designed as adjustable racing car dampers, with which the driver can manually select proper damping value for varying driving conditions. These dampers were selected for the test, because the physical dimensions, force characteristics, available coil spring set, price of the components and the delivery time were sufficient for the goals of this research work.

The MR damper/coil spring set was first tested separately in a hydraulic loading frame. In this test the components were loaded with a hydraulic cylinder using sinusoidal and saw-tooth waveforms to characterise the dynamic and static properties, such as the function of MR control voltage, motion speed, frequency, and temperature.

In Figure 8, the single damper force characteristics are presented as a function of motion speed with the MR control voltage as parameter. The results are given for two different damper configurations. The dashed lines represent the original damper and the solid lines are for the damper after modifications, which included change of MR fluid (to one with larger yield stress, but about the same viscosity as the original) and some modification in the flow gap size of the MR

valve. The purpose of these alterations was to make the minimum force of the damper as small as possible, without compromising too much the maximum force characteristics as a function of MR control voltage (magnetic field). The results for the modified damper are represented by the solid lines in Figure 8.

The actual vibration suppression performance tests were carried out twice: Firstly using the original MR dampers and then with the modified dampers. The original dampers were clearly too "stiff", i.e., the minimum damping force (without control input) as a function of motion speed was too large for the semi-active control algorithms to show any performance better than that measured in the passive state of MR damper operation (zero control input).

The damping performance with the modified dampers and semi-active skyhook control are shown in Figure 9. Only rather small improvement in the vibration suppression performance was achieved, while comparing third octave spectra in passive operation mode and semi-active case for measurement location at the rear corner of the cabin. The results for the fuzzy control algorithm are similar to the skyhook results.

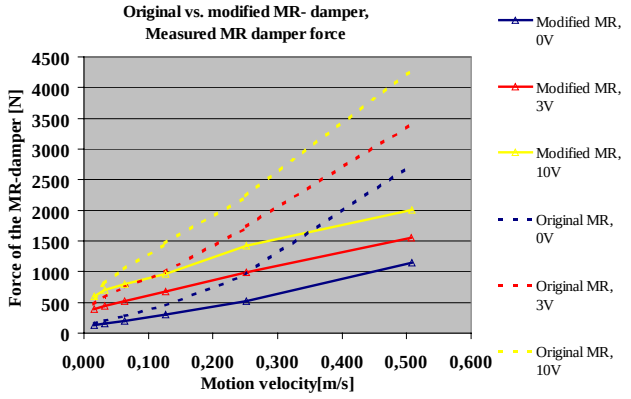

Figure 8. Damper force characteristics as a function of motion speed for the original (dashed) and modified (solid) dampers. Three MR control input voltages per case (0V, 3V and 10V).

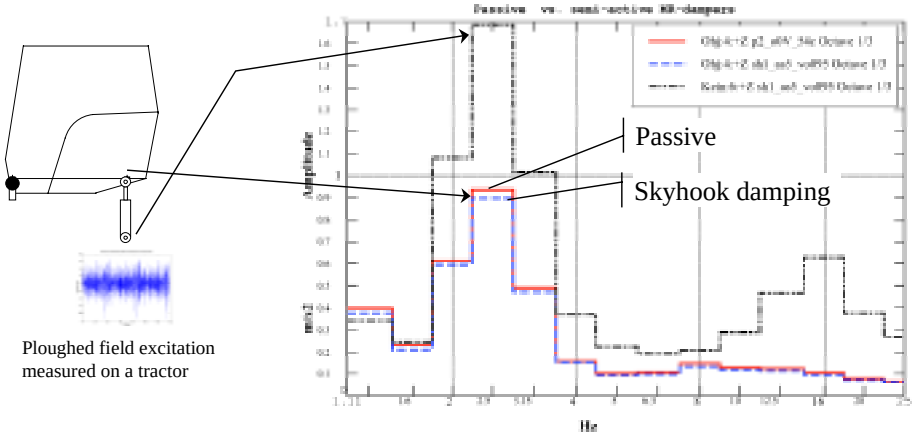

Figure 9. Measured third octave acceleration spectra for base excitation (dash-dot line), passive operation mode (solid line) and skyhook damping (dashed line). Modified MR dampers.

6. How to improve performance?

The reason for poor vibration suppression capability of the MR damper/semi-active control combination were studied using the 1-dof MATLAB/Simulink model, which was built to simulate the ideal skyhook damping. The measured damper force behaviour (Figure 8, solid lines) was input to the simulation model and responses for the ploughed field excitation were calculated. Figure 10 shows the third octave acceleration spectra for the response of the 1-dof system in the passive and semi-active skyhook control modes of operation of the modified MR damper. The vibration suppression performance of the simulation results was similar to that measured in the laboratory test bench. This result indicates that the achieved vibration damping effect could not be better than measured, and suggests that the damper force properties are far from optimal for the semi-active control.

Some results from further studies on the effect of minimum force characteristics of a MR damper are shown in Figure 11. Here the force behaviour of the modified damper is changed by setting the force at zero control voltage to vary within a range of 50–200 N for a motion speed range of 0-0,5 m/s. In other respects the characteristics are the same as in the case considered in Figure 10. The spectra in Figure 11 shows clearly how the acceleration response of the 1-dof system (black solid line) is greatly reduced compared to the performance obtained with the modified damper in the passive mode of operation (blue solid line, zero control voltage). This relatively simple simulation study neatly demonstrates the importance of the minimum force characteristics of MR dampers (or any other damping device) for the effective vibration suppression whenever semi-active skyhook control or algorithms based on assumptions of skyhook principle are used.

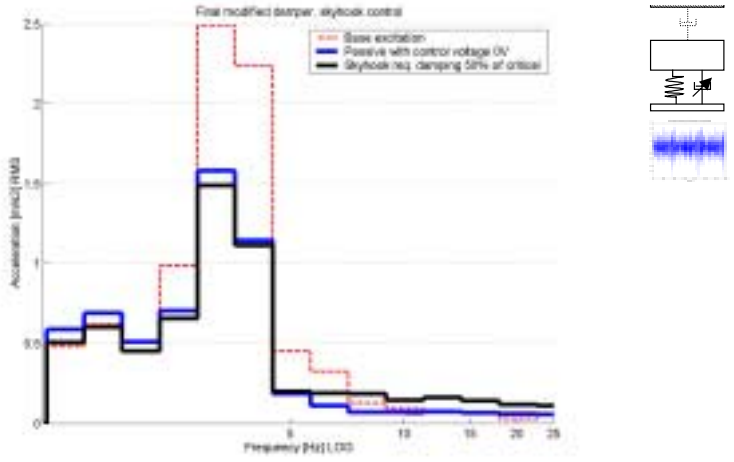

Figure 10. Simulated third octave acceleration spectra for base excitation (dash-dot line), passive operation mode (solid blue line) and skyhook damping (solid black line). Force characteristics of the modified MR damper.

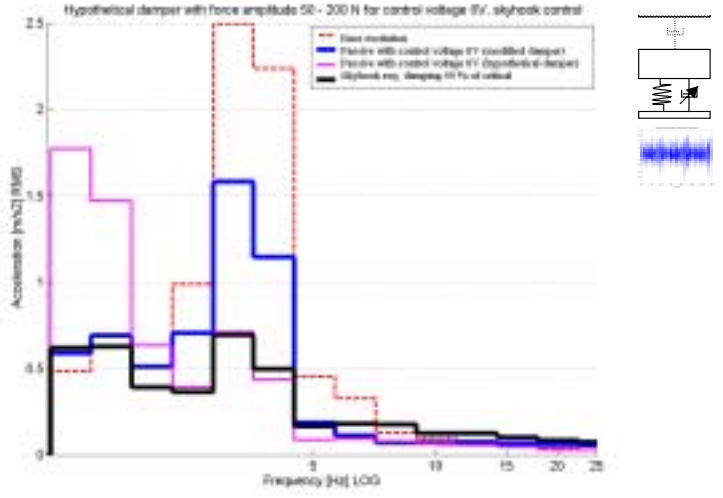

Figure 11. Simul ted third octave acceleration spectra for base excitation (dash-dot line), passive modified damper (solid blue line, as in Fig. 10), passive hypothetical damper (solid pink line) and skyhook damping (solid black line). Force characteristics of a hypothetical modified MR damper with force at zero control voltage set into range 50–200 N.

7. Discussion and conclusions

In the normal operational conditions of a mobile machine it is common for the driver to be subject to rather severe vibration loading. This fact has encouraged vehicle manufacturers to develop at least passive damping systems for seat, cabin and axle suspensions. In addition, active and semi-active vibration control products and prototypes have also been built in Finland (Vessonen et al., 2000).

Passive suspension systems reduce the vibration only in certain frequency bands and amplify other frequencies, so compromises have to be made in the design process. In order to avoid unwanted response amplification within the resonance frequency range of the suspension, the price to be paid is to increase the response at higher frequencies. The good news is that with careful design, noticeably reduced vibration responses can be achieved, as compared to the situation without any damping system.

A semi-active suspension system can be considered a good compromise between passive and fully active systems. As the simulation results of this study show, with semi-active system it is possible to attain considerably better vibration suppression performance than using passive solutions. The suspension properties can also be tuned and optimised for varying operational conditions. For example, in a simple case it is possible to have preset, stepwise changeable damping properties, perhaps with temperature change compensation (oil, viscosity), for various driving conditions. A more advanced system would include continuous damping force adjustment with proper control algorithm such as skyhook or fuzzy control method, considered in this study.

With an improved and more comfortable working environment it is possible to end up in situation, where the driver, in rough driving condition, can lose the touch to the real loading of the vehicle, because of the reduced vibration exposure. In order to avoid this kind of overload situations, plus possible structural damages, it is possible to use semi-active (and also fully-active) suspension system to restore the touch, if the going gets too tough.

The MR fluid-based damper is a very promising piece of hardware technology for implementing semi-active vibration control systems for vehicle cabins, seats

and axles. These dampers are relatively simple devices with a fast response time and large damping force with good dynamic range can be controlled with a small amount of external energy.

Unfortunately, it was not possible in practise to fully demonstrate the effectiveness of MR dampers and associated control schemes in the present study. This was due to the minimum damping force characteristics of the selected commercial MR dampers. The force level with zero control voltage to the damper was simply too large e.g., for the skyhook scheme, which requires damping force to be zero in some situation, in order to achieve good vibration control performance. Despite of a good effort to modify the force properties of the damper, a satisfactory minimum force characteristic could not be achieved. However, on the basis of the knowledge gained, it is quite evident that proper damper force behaviour can be realised with careful design and implementation of MR fluid and MR valve including relevant coil assembly.

Altogether, the conclusion is that the MR fluid-based semi-active vibration control system is a feasible new technique with promising features for various suspension needs in mobile machines, for which better performing cost-effective alternatives for rigid joints and passive suspensions are needed.

References

Karnopp, D., Crosby, M. J. & Harwood, R. A. 1974. Vibration Control Using Semi-Active Force Generators. Journal of Engineering for Industry, May, pp. 619–626.

Vessonen, I., Järviluoma, M. & Nevala, K. 2000. Modern design and active control methods in mobile machine vibration control. In: Airila, M. et al. Smart Machines and Systems – Recent advances in mechatronics in Finland. Espoo: Helsinki University of Technology, Publications in Machine Design.

Vähänikkilä, A. 2001. Fuzzy control of semi-active front axle suspension of an agricultural tractor. Master of Science Thesis, University of Oulu, Department of Mechanical Engineering. (In Finnish)

Active Vibration Control of Rotor – Test Environment with Non-Contact Magnetic Actuator

Kari Tammi
VTT Industrial Systems
Espoo, Finland

Abstract

The goal of this work was to set up a test environment for active vibration control of rotors, to study the dynamics of the system, and to design a control system to control the rotor vibrations. The principal idea was to control vibrations with a non-contacting magnetic actuator without a load-carrying function. The rotor was supported by conventional bearings at its ends. The test environment consisted of a rotor test rig, a magnetic actuator, and a programmable control unit. The test environment was tailored to have a large response when running the rotor close to its bending critical speed. First, damping the system by using a simple velocity-feedback controller was studied. The parameters of the controller were defined experimentally from the measured data. According to the simulations and the experiments performed, the velocity-feedback control system reduced vibration levels significantly. The controller made it possible to run the rotor over the critical speed. Second, a feedforward system, based on an adaptive finite-impulse-response filter, was designed to compensate disturbances due to mass imbalance. The coefficients of the filter were adapted by a least-mean-squares algorithm. The response due to mass imbalance in the rotor was significantly decreased. The simulations and experiments showed that the adaptive filter could be used as a supplementary system to the feedback system.

1. Introduction

The principal concept of this work was to study how to control vibrations of a rotor supported by conventional bearings by using a non-contact electro-magnetic actuator. The work was in particular focused on such applications that were not potential active magnetic bearing applications, due to the fact that several heavy rotating machine manufacturers exist in Finnish industry. The electro-magnetic actuator was chosen because electronics were used more frequently in contemporary actuators, sensors, and control systems. Even when speaking of heavy machine design, the test environment was designed to be simple and on a small scale. This was an important issue, since basic rotordynamic phenomena could be studied and simple control systems could be implemented quickly and safely. Implementing the ideas into a machine out of the laboratory and extrapolating the phenomena to a larger scale will require effort and further research. Nevertheless, this environment was a perfect start.

The aim of this work was to construct a test environment for the active vibration control of rotors, to study its dynamic behaviour, and to design and test active vibration control systems. The systems employed had to decrease the displacement response in the rotor and increase the operational range of the test system over its critical speed. The requirement of adaptivity was set for the control system to be designed. This work was designed to be a step towards the definite goal of developing an intelligent control system for heavy rotating machines. Therefore, the work was aimed to study applicability of the test environment, to relate the results to practice, and to direct forthcoming research.

1.1 Rotor kit

The rotor kit consisted of a rotor 10 mm in diameter and 560 mm long, which was supported by journal bearings (Figure 1). The weight of the rotor shaft was 350 g. The torque from the electrical motor to the rotor was transmitted by means of a flexible coupling. The radial displacements of the rotor could be measured in two projections with eddy current transducers. The bearings, the displacement transducers, and the electrical motor were all fixed to the V-shaped

body in such a way that they were easy to move and detach. The rotor kit included two movable and detachable disks that could be fixed to the rotor in any spot. These adjustments made the dynamic behaviour of the system very straightforward to customise.

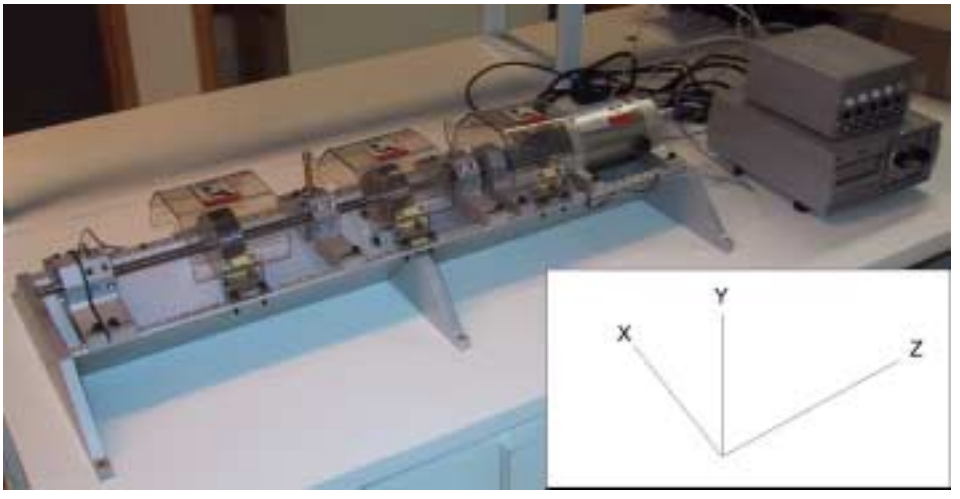

Figure 1. The rotor kit in its basic configuration. The control box and the transducer output box piled on the right in the picture. Note the co-ordinate directions used in this work.

1.2 Actuator

The body of the actuator was composed of stamped iron sheets welded together. The body had eight teeth forming the iron core for the radially located horseshoe magnets. The outer diameter of the body was 100 mm and the inner diameter was 50 mm. The actuator was fixed to the rotor kit body by means of an aluminium mount. A counter-part, also a laminated disk pack, was fixed to the rotor shaft. The outer diameter of the cylindrical counter-part was 47.5 mm, its length was 65 mm, and its weight was 760 g. Hall transducers were glued onto each tooth in order to measure the magnetic flux density in the air gap. This was to measure force induced to the rotor. The vibration amplitude of the rotor was mechanically restricted to prevent the rotor hitting the Hall transducers.

1.3 Control unit

The control unit was modified from an active magnetic bearing control system. Amplifiers to control currents, a programmable signal processing hardware, inputs, and outputs were all integrated into the control unit. The hardware and the software in the control unit were modified for the purpose. A spot to apply the control systems for our purpose was pointed out in the code. The procedures to produce the control forces were available in the control unit. The control system to be designed would determine the force required and feed the force commands to the force control loop (Figure 2). The force control loop was run using either the flux feedback or the current feedback. The flux signals were provided by the Hall transducers. The current signals were measured in the amplifiers.

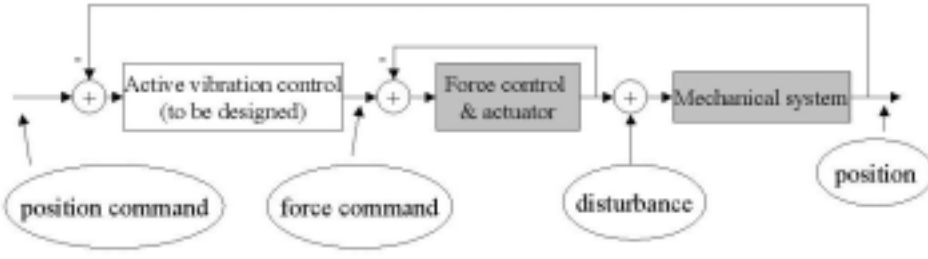

Figure 2. The control system to be designed was to feed the force commands for the force control loop.

2. Materials and methods

2.1 Jeffcott rotor

The Jeffcott is presented in Vance (1987), for example. It consists of a flexible shaft with zero mass, supported at its ends. The supports are rigid and allow rotation around the centre axis of the shaft. The mass is concentrated in a disk, fixed in the middle of the shaft. The system is geometrically symmetric in its rotational axis, except for a mass imbalance attached to the disk. When rotating,

the mass imbalance provides the excitation to the system. For the Jeffcott rotor, the equation of motion is described by

$$m\ddot{z} + c\dot{z} + kz = m_u r_u \omega^2 e^{i\omega t}, \quad (1)$$

where on the left side of the equation, m is the mass of the disk, c is the damping constant representing an external source of damping, k is the spring constant, equivalent to the stiffness of the shaft, and z is the complex variable representing the position of the centre of the disk. The real part and the imaginary part can be understood as orthogonal co-ordinates of the position of the disk. The symbols $\ddot{z}$ and $\dot{z}$ are the second- and first-time derivatives of the position variable. On the right side of the equation, m_u is equal to unbalancing mass, r_u is the distance of unbalance from the geometrical centre of the rotor, ω is the rotational speed, i is the imaginary unit, and t is the time variable. In this work, the critical speed refers to the speed that was equal to the natural frequency of the Jeffcott rotor[1]. The test environment was tailored to represent the Jeffcott rotor by locating the cylindrical part in the middle of the slim shaft. The Jeffcott rotor was considered as two separate one-degree-of-freedom systems (Figure 3). One system was considered to vibrate in the horizontal (X) direction and the other system in the vertical (Y) direction. The actuating point of the force and the placement of the displacement transducer were approximately collocated.

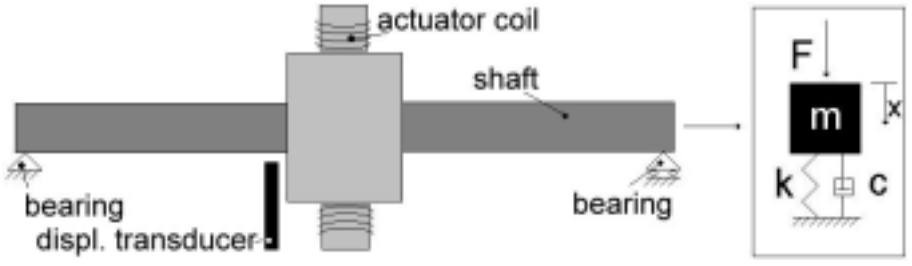

Figure 3. One direction of the rotor-actuator system was simplified to a one-degree-of-freedom vibrator. The other direction formed another similar system.

[1] In literature, the critical speed could also the speed at which the maximum response occurred.

2.2 Dynamical characterisation

The modal analysis was performed in order to estimate the modal parameters of the mechanical system and to validate the assumption on the Jeffcott rotor. The measurements were carried out on the non-rotating rotor in both vertical and horizontal directions. The first bending modes occurred 43 Hz in both directions, equivalent viscous damping being about 2%. The second modes were equal to 296 Hz (horizontal) and 297 Hz (vertical), the damping being about 2% for both. The results corresponded to expectations; the lowest modes had a relatively low frequency, while the second modes had clearly higher frequencies. The open-loop responses were measured in order to identify the mechanical system, the actuator, and the control system together. This was to define the system parameters and again validate the assumptions of the Jeffcott rotor. The measurements were carried out by exciting the rotor with the magnetic actuator. The force was induced in the middle of the bearing span and the displacement measured from the same point to be used in active control. The force was swept from 5 Hz to 400 Hz and the measurements repeated with several rotational speeds. The results showed a slight decrease in the natural frequencies of the first bending modes, being equal to 40 Hz. The parameters *m, c,* and *k* for the one-degree-of-freedom vibrator model were computed from the parameters achieved in the measurements. The measurements led to the spring constant $k = 33333$ N/m, mass $m = 0.528$ kg, and the damping constant $c = 2$ Ns/m (Figure 4).

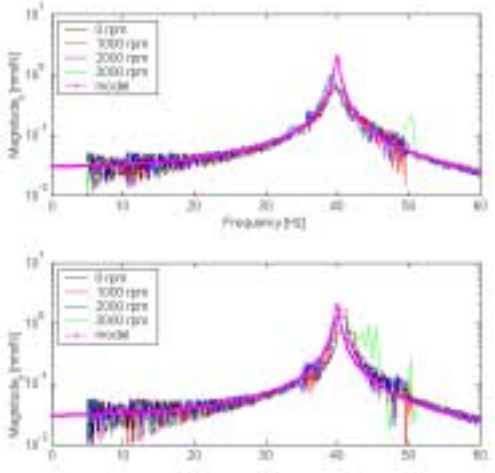

Figure 4. The measurements with different rotational speeds were compared to the model. Note the logarithmic scale in the magnitude.

2.3 Feedback control

The design of the control system was divided into two parts. First, a feedback control system was used to reduce system response over a larger frequency band. Second, a feedforward system was used to compensate an excitation due to rotation. For a one-degree-of-freedom vibrator, the transfer function from a force to displacement can be expressed as

$$H_{ol}(s) = \frac{1}{ms^2 + cs + k}, \tag{2}$$

where s is the Laplace variable, m corresponds to the vibrating mass, c is the damping constant, and k is the spring constant. The function H_{ol} refers to the open-loop transfer function. The closed loop transfer function with velocity feedback is

$$H_{cl}(s) = \frac{1}{ms^2 + (c + K_d)s + k}, \tag{3}$$

where K_d equals the derivative gain. The magnitude of response at the resonance can be determined by selecting an appropriate derivative gain. For example, the requirement for the characteristic equation of the closed-loop system

$$ms^2 + (c + K_d)s + k = (-\lambda - i\lambda)(-\lambda + i\lambda), \quad (4)$$

where λ is a positive constant and i is the imaginary unit, is one way to place the closed-loop poles leading to 'good behaviour' or 'nice responses' of a system (Glad & Ljung, 2000). Derivation as an operation was prone to high-frequency noise. A low-pass filter was designed, to restrict control actions in a certain bandwidth[2]. Equation (4) led the derivator gain of 186 Ns/m and the poles at ($-178 \pm i\ 177$) rad/s. According to the simulations, the designed feedback system significantly reduced the vibrations in the rotor. Two feedback control systems were implemented in the control unit; one controlled the vertical direction, and the other controlled the horizontal direction. No coupling between the degrees of freedom was assumed.

2.4 Feedforward control

A feedforward control system, based on the use of a reference signal to derive control actions, was used to compensate excitation due to rotation. The reference signal was generated from the rotational pulses measured. An adaptive FIR[3] filter was used to estimate the correct amplitude and the correct phase with respect to the compensation signal and the mass imbalance in the rotor. The output of the filter, *u(n)*, is the sum of I pieces of input pulses multiplied by the coefficients h_i

$$u(n) = \sum_{i=0}^{I-1} h_i \cdot x(n-i), \quad (5)$$

[2] The bandwidth of the produced counter-force was also limited by the bandwidth of the actuator.

[3] Finite Impulse Response or non-recursive filter.

where *x(n)* is the input pulse queue, *I* is the order of filter, and *n* is the index pointing to the latest pulse in the pulse queue, and *n-i* represents a shift backwards by *i* pieces of pulses in the pulse queue. The pulse queues presented are formed of sampled real signals. The LMS[4] algorithm was used to adapt filter coefficients. The coefficients h_i are updated by using the equation

$$h_i(n+1) = h_i(n) - \alpha e(n) r(n-i), \tag{6}$$

where α is a convergence coefficient, *e(n)* is the error to be minimised, and *r(n-i)* is the reference signal filtered with a model of the system to be damped. (Fuller et al., 1996).

The simulation model was built together with programming the algorithm into the control unit because boundary conditions set by the control unit had to be taken into account. A filter order of 12, an update frequency of 500 Hz, and a maximum convergence coefficient of 0.01 were selected. The simulation indicated the algorithm to be working with a remarkable reduction in the response of the system. As to the feedback system, two algorithms were implemented in the control unit; one worked in the horizontal direction, the other in the vertical direction.

3. Results

The control systems discussed were programmed into the control unit and tested in a test environment. First, the results were measured using only the feedback control. Second, the results were measured when both algorithms, the feedback and the feedforward control were functioning. The responses were measured with the same transducers as were used for the active control. The data was sampled with a sampling frequency of 2048 Hz.

[4] Least Mean Square algorithm.

3.1 Feedback control

Figure 5 shows the displacement signals measured in a run-up condition. The run-up was performed from 4.2 Hz (250 rpm) to 65 Hz (3900 rpm) with a rate of 16.7 Hz/min (1000 rpm/min). The active control was switched on at 38 Hz, right before crossing the critical speed. The active control was switched off at 52 Hz. In the beginning of the run-up, rotational speed being less than 20 Hz, the response was on the order of 20 microns (peak). From 20 Hz to the switch-on point of the active control, vibrations increased on the order of 180 microns before the switch-on. The active control reduced the response on the order of 20 microns until it increased to about 50 microns at the switch-off point of the active control. The second multiple of the rotational frequency also excited the resonance frequency, as can be seen from the vertical response at 20 Hz in Figure 5.

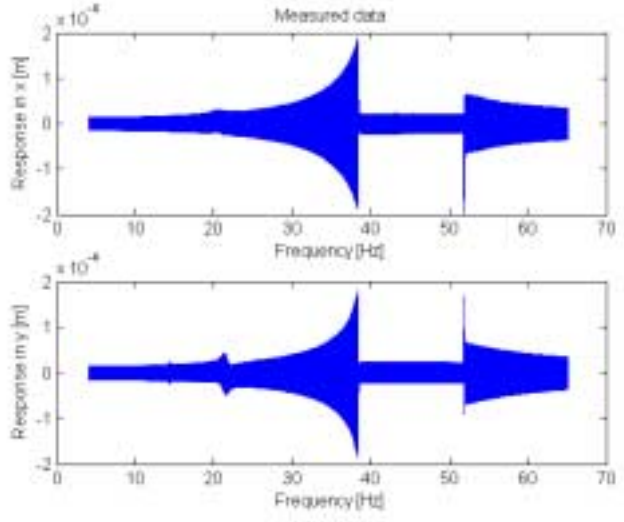

Figure 5. The measured response is shown as a function of the rotational frequency. The vibration in the horizontal direction (above) and the vertical direction (below) were reduced significantly when the controlled was switched on before crossing the critical speed.

3.2 Feedforward control

The tests with the feedforward control were carried out starting from the rotational frequency of 11 Hz. The response during the switch-on period of the filter is shown in Figure 6. The rotor was running at the critical speed with the feedback control alone when the adaptive filter was switched on. After the switch-on, the response was decreased from order of 30 microns to 2 microns in about 1.5 seconds The rotational speed was 40 Hz (2400 rpm) and the convergence coefficient was equal to 0.01. Analysis in the frequency plane showed that the harmonic vibration induced by mass imbalance was almost completely compensated. Comparison between the non-controlled and the controlled cases showed that the first harmonic was attenuated mainly due to the feedforward loop. Contrary to this, the vibration at natural frequency was damped by the feedback loop. The active control also had a slight damping effect on the higher harmonics. Figure 7 shows the responses in the horizontal and vertical direction during the sweep from 11 Hz to 65 Hz. The response decreased from 5 microns to 2 microns when the rotational was swept from 11 Hz to 18 Hz. From 18 Hz to 45 Hz, the response was approximately constant, being on the order of 2 microns. Above 45 Hz, higher peaks in response occurred randomly. The highest peak observed was 42 microns in the vertical direction. A correlation with the peaks in the quality of the reference signal was observed. The reference signal had a discontinuity at the same instant than a peak occurred. The control commands by the feedback control and by the feedforward control were recorded separately. Figure 8 shows the control command as a function of time when the rotational speed was 25 Hz. The control commands computed in the feedback loop were characterised by one sinusoid at 25 Hz if the feedforward compensation was off. The control commands by the feedback loop were decreased when the feedforward compensation was switched on. This was due to the sinusoid at 25 Hz being compensated by the feedforward loop. Table 1 shows the rms values of the control force commands and corresponding displacements at three rotational speeds. In the case of feedback control only, the magnitude of the feedback force was from 0.9 N to 2.1 N. When using the feedforward control, the magnitude of the feedback force was reduced by about half. The examination showed that total control force was not increased when using the feedforward compensation even when the response was significantly reduced.

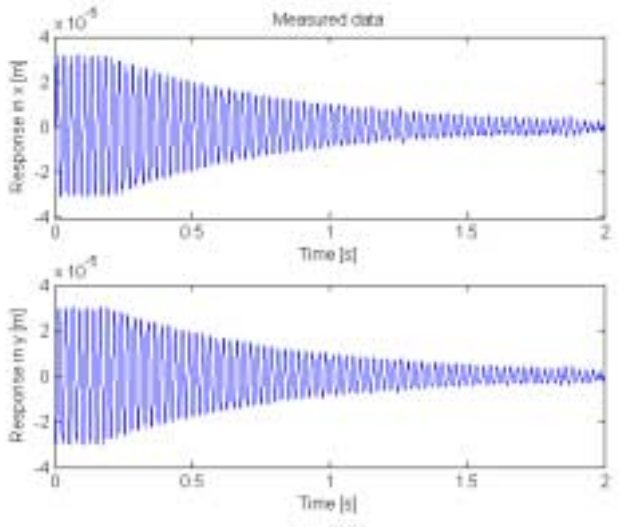

Figure 6. The response in the X-direction (above) and Y-direction (below) were measured during a switch-on period of the FIR-filter. The feedback control was running alone in the beginning of the time record. Then the adaptive FIR-filter was switched on.

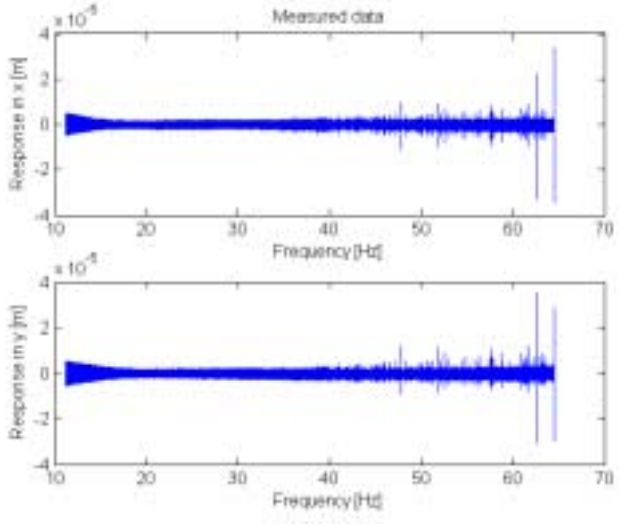

Figure 7. The responses were measured during the sweep from 11 Hz to 65 Hz.

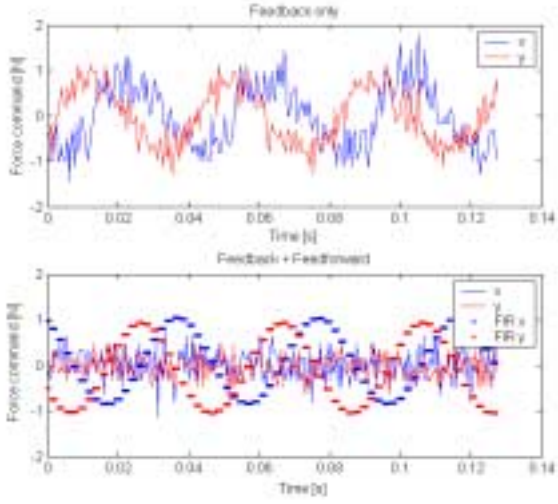

Figure 8. The commands for the control forces were recorded when using the feedback control only (above) and both control algorithms (below). The rotational speed was 25 Hz. The phase between the subplots should not be compared since the measurements were not triggered from the rotational pulse or displacement.

Table 1. The results of control force commands and the displacements are shown below (rms-values).

Rotational speed		FB control only		FB + FF control together			
		FB force	Displacement	FB force	FF force	FB+FF	Displacement
[Hz]	[rpm]	[N]	[microns]	[N]	[N]	[N]	[microns]
25	1500	**0.9**	26.2	**0.4**	**1.0**	**1.1**	1.2
40	2400	**1.4**	27.6	**0.6**	**1.3**	**1.4**	1.1
65	3900	**2.1**	24.1	**0.9**	**2.3**	**2.5**	1.5

4. Discussion

The vibrations were successfully damped with the velocity feedback control. The attenuation was the largest at the critical speed, but it was significant in the frequency band from 15 Hz to 80 Hz. In the whole frequency band of interest, an approximately constant displacement response was achieved by using the feedback control. The adaptive feedforward compensation attenuated the

disturbance at the frequency of rotation. In addition to the feedback control, the feedforward control decreased the displacement response on the order of microns. With feedforward control, higher peaks occurred randomly with the rotational speeds higher than 45 Hz. The reason for this behaviour was not completely clear; it could be due to an inappropriate choice of filter parameters or rotor dynamic phenomena. The length and update frequency of the filter were selected in such a way that the compensating signal was coarse at high frequencies. This produced high frequency components that could have excited the rotor. The explanation due to the rotor dynamic phenomena rested on the fact that a super-critical rotor rotates around its centre of gravity whereas the compensation forced the rotor to rotate around its geometrical centre.

The different roles of algorithms were pointed out. The feedback control added viscous damping to the system and provided smooth response in the frequency band. The feedforward control compensated the greatest source of excitation that occurred at the rotational speed. The comparison between forces computed by different control algorithms showed that the magnitude of the force did not increase even as the response decreased significantly. The selected test environment was suitable for the purpose in terms of flexibility and functionality. The rotor kit was easy to modify and good for demonstration purposes. The control unit was found to be a flexible and robust device with a well-organised user interface.

References

Fuller, C. R., Elliot, S. J. & Nelson, P. A. 1996. Active control of vibration. Academic Press. London. 332 p. ISBN 0-12-269440-6.

Glad, T. & Ljung, L. 2000. Control theory. Taylor & Francis. London. 467 p. ISBN 0-7484-0878-9.

Vance, J. M. 1987. Rotordynamics of turbomachinery. John Wiley & Sons, Inc. USA. 388 p. ISBN 0-471-80258-1.

Active Fatigue Damage Control

Mikko Lehtonen [1)], Risto Laakso [1)], Mikko Savolainen [1)], Jaakko Säilä [1)],
Risto Hedman [2)]
[1)] VTT Industrial Systems, Espoo, Finland
[2)] Emmecon Ltd., Lappeenranta, Finland

Abstract

In the 'Fatigue damage control' project within VTT's 'Smart materials and structures' research programme, it was studied how to implement a machine that independently observes fatigue damage. A machine monitors itself and its environment. Based on that information, the machine changes its behaviour. For example, the machine could measure strains for damages and damage rates. After that, the machine can decide whether to modify its behaviour, trigger an alert, etc.

1. Introduction

A machine that has active durability control could be like the machine in Figure 1. The application must be one that has a limited fatigue life and behaviour that can be changed. A typical application could be mobile boom structures such as mobile cranes and forest harvesters. Making these structures smart primarily means they would get automated functions along with structural health monitoring (SHM). In this context, 'process' means the total control of the structures described above, with the control system being a combination of SHM and automation. The control system is realised with custom electronics and software capable of sensing the structure and controlling the actuators in it.

The main purpose is not to run the process without an operator, but to help the operator control the process better. In this concept, the geometry, movements, and loads are continuously controlled, and the control system is ready to limit the movements when there is an increase in the probability of overloading, a

decrease in stability, or an increase in the damage rate. This new approach will offer the following advantages:

- In the design phase, the safety factor of the structure can be reduced because the integrated control system will not allow overload or wearing operations. Material costs will be reduced in the manufacturing phase.
- In use, the personal characteristics of the operator are not as important as they are with traditional designs, and the operator does not need to be highly skilled. Salary costs are reduced and safety is enhanced.
- The structural loads are controlled continuously. This will reduce the damage rate of the structure and increase its stability, which will further increase the safety and lifetime of the equipment and reduce service costs.

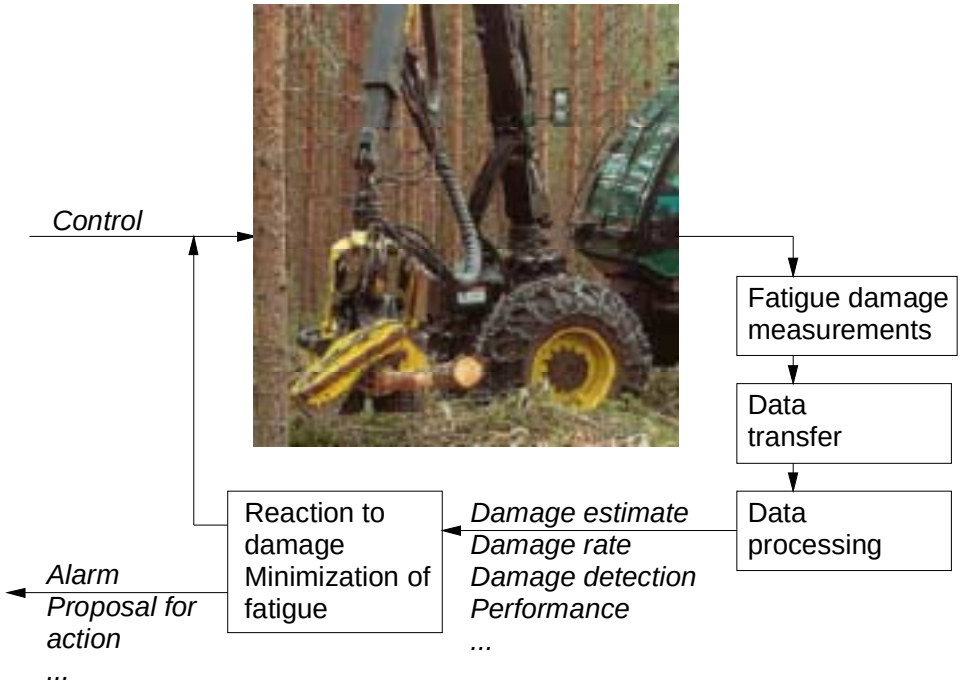

Figure 1. Active fatigue durability control.

2. Measuring methods of a fatigue damage

Two types of approaches, or a combination of these types, can be used when monitoring the condition or state of a structure. Structural damage can be estimated using S-N curves, local strain method, fracture mechanics, or a combination of these. The calculated estimates are typically very conservative.

Damage can also be observed by monitoring changes in the structure. This important method is much more accurate, but difficult to apply because very early detection of cracks may be impossible in some cases without the help of a human.

It's obvious that in some cases estimated damages or damage rates are way too conservative for an adaptive reaction process (Figure 2). However, calculated estimates are needed for minimising fatigue damage. Instead of adaptiveness, if we use a directive reaction process, we might rely only on S-N curves and probability calculus. If we combine those with hydraulic pressure, heat, forces, velocity and/or acceleration data, for example, we could get a good view of what's going on and what should be done. But in that way we get only an alarm or maintenance instructions, and those belong to a common monitoring system. The directive reaction process is only part of a true intelligence system with feedback and many embedded control loops operating without the aid of the user.

Reliable detection of a crack and observation and prediction of its growth rate enable adaptive and learning processes as well as directive reactions. In active durability control processes, it is very important to detect cracks before they grow too large or too quickly and the structure becomes unreliable. In addition, the decision module must be able to process the data very fast and effectively in any conditions of the structure. The module can include, for example, neural networks, fuzzy logic, case-based reasoning, different types of optimisation methods, rule-based systems, and other methods related to artificial intelligence.

Each method of measurement has its own uncertainties in measurement and calculations. Refining the measured data into a more useful form is often done without any statistical methods, even though every computation includes potential sources of error. The system can also monitor uncertainties and

conditions of the sensors. The errors made in measurements must always be estimated. Of course, the real values are not the measured ones; they are the measured data subtracted by the error (Laakso & Savolainen 2002).

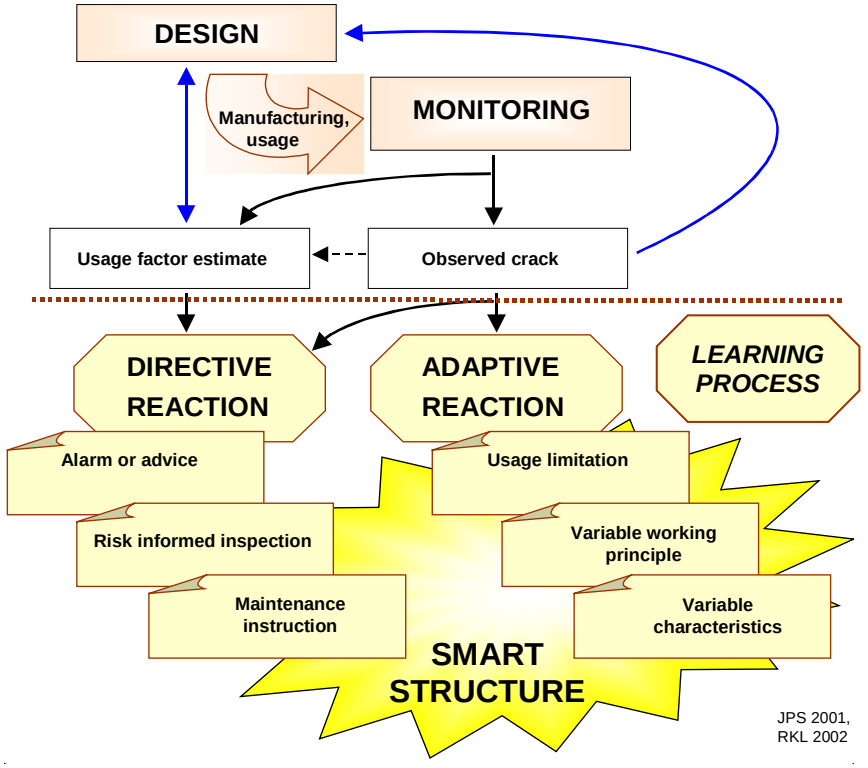

Figure 2. Some aspects of monitoring and solutions of the smart structures in fatigue durability control.

Some of the measurement technologies developed for regular inspections could also be suitable for real-time monitoring, but usually the technologies that are simple to automate are used because of practical and cost reasons. Are the chosen methods reliable enough (even in field measurements), and what is the probability of detection? Note that even in thorough NDT inspections, the probability of detection is always finite – a fact which has not often been considered. If the measured data is relevant, can it be determined when fatigue damage occurs, and what are the time- or state-dependent limits of error (Figure 3).

Tables 1 and 2 show measuring methods and some of their advantages and disadvantages, discussed previously in the Durability Control project (Laakso et al. 2001). “Extent” means the typical size of an observed area: 1 = a few square centimeters; 2 = stress concentration; 3 = component; and 4 = whole structure.

Table 1. Calculating fatigue damage.

Method	***Extent***	***Disadvantages***	***Advantages***
Strain gauges	3	Installation errors, need of calibrations	Proven technology
Fiber optic Bragg Gratings	3	Cost, signal processing	Passive, immune to electromagnetic disturbances
Fatigue fuse	2	Only an on/off indication, assumes that the fuse and the structure behave similarly	Low cost
X-ray diffraction	3	Proven only in laboratory environments	Scientifically based

Table 2. Observing fatigue damage.

Method	***Extent***	***Disadvantages***	***Advantages***
Foils, coatings	4	Needs smooth surface, partly unknown technology	Simple, low cost, new
AC and DC potential drop	2	High cost, difficult to apply to structures	Proven technology, verification
Strain gauges	1	Coverage, interpretation	Simple, low cost
Grids, fibers	3	Coverage, high cost	Simple, on-line
Structural frequency response changes	3	Sensitivity, calibration	Common technology, reliable
Local compliance changes	1	Small coverage	Simple, low cost
Ultrasonics	2	High cost, coverage	Technically verified
Acoustic emission	4	Difficult to interpret, passive	Proven technology, verification
Eddy current	2	Calibration, coverage	Proven technology, verification

Figure 3. Some of the difficulties and questions within the fatigue damage detection of smart structures.

3. Measurement data processing

One can easily get a damage estimate if a common and simple monitoring system is used. The system can observe relevant quantities and calculate crack growth or damage rates, for example. The data processing usually includes at least a rainflow algorithm with fixed S-N curves and relevant data factors. An embedded vibration analysis can also be very useful. The machine must react if the measured (or calculated) data exceeds the given alarm levels, the data shows flat responses or unexpected spikes, no data exists, or the sensors do not agree with the data findings.

When a continuous phenomenon is measured, it is always made discrete. It is not useful to use only recorded data, which still might be needed for backup purposes. In real-time monitoring and fatigue minimisation, primarily the direct data flow coming from the sensors is used. Some of the data findings are expected and true – some are unexpected and might also be erroneous, which must be taken into account in data filtering, selection, and analysis. In some of the smart structures and durability control cases, there should be two different

procedures: one for the data, which is ranked to be true, and another for the cases in which the data is (or might be) spurious.

An intelligent structure with a durability control system can use the measurement data – observations or estimations – only if the data is in proper format for further data processing modules. The crack size or the amount of the remaining lifetime could be one output of the data processing module, which could include several sub-modules (Figure 4). The first sub-module – pre-processing – mainly includes all functions between the sensor and the data scaling. The second sub-module includes an actual processing phase, where the pre-processed data is formatted, analysed (Figure 5), and selected to meet the requirements of the overall system.

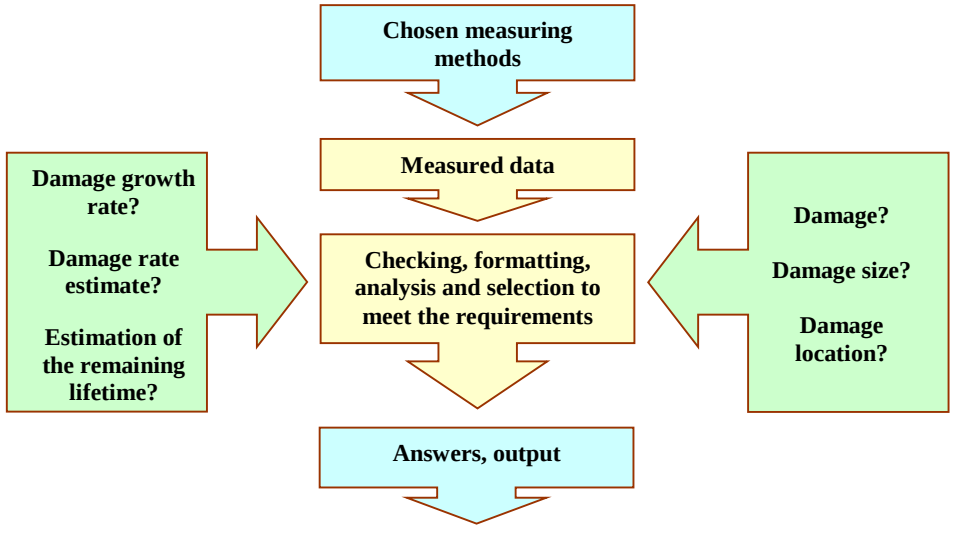

Figure 4. How is it possible to get intelligent durability control related solutions from the measured data of the chosen measuring methods?

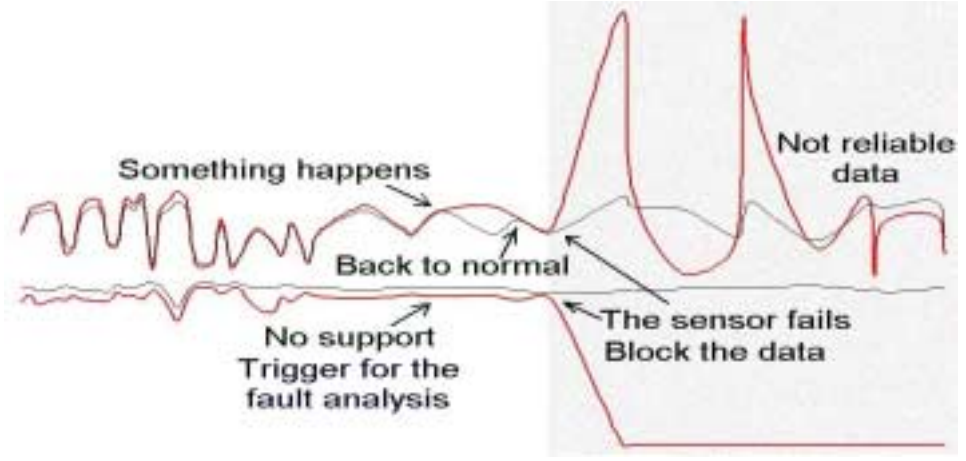

Figure 5. When a sensor fails, it no longer produces comparison values with other sensors. The data (red line) must be removed from any further analysis.

4. Measuring and control electronics

In this chapter, a mobile boom structure is used as an example. To implement the smart ideology into mobile boom structures, the co-ordinate control concept can be realised. The directions of the movements given by the driver or semiautomatic process cycles have to be transformed into the movements of the joints. This task is done by the interpolator, which calculates new values for joints every 'interpolation interval'. Between these intervals, the joints, or axles, try to keep the speed (or position) they were commanded to keep in the previous 'interpolation interval'. Each joint executes this task independently and calculates new values for the joint actuator every control interval. At every control interval, the processor realising this control loop reads the position of the joint, calculates its speed (with the previous position value), compares this speed to the speed commanded by the interpolator, and scales the difference between actual and set values to be output to the servo amplifier controlling the joint actuator. The interpolation interval is one or more decades longer than the control interval.

The joint position sensor has to be sensitive and withstand the harsh environment of mobile boom applications. The sensitivity requirements are defined by the geometry of the equipment. It's not exceptional that there is an

angular joint with a 5m boom connected to it. In this case, a 2” angular movement will cause a 3mm linear movement in the tip of the boom. This 2” is an angular accuracy one can reach with a ‘leading edge’ resolver and electronics in optimal conditions – the resolution of the regular technology is worse by a decade. On the other hand, the structures’ elasticity will probably cause a deviation larger than the one caused by the lack of the resolution of the sensor. The structural control also has built-in tools to control deviations of the structure; the sensor resolution cannot be improved by thricks.

The structural control measuring system should be connected to the interpolator of the control system.

The control and sensing system can be centralised or distributed. Traditionally, the centralised approach is used, in which one computer with several processes is running the system. In the distributed approach, several small computers run one or a few tasks each (Figure 6). These small computers run their tasks independently and are connected to a network for assigning tasks and distributing information between the computers. Figure 6 illustrates the principle of a distributed measuring and control system.

A fieldbus is one member in the family of local area networks (LAN). CAN (Controller Area Network) is a fieldbus widely used in vehicles such as personal cars, trucks, and cranes. Via the CAN, various small computers (micro-controllers) located around the equipment can send messages to each other. Here is a simple example:

- The dashboard computer will recognise that the turning light switch is turned to the right.
- The dashboard computer will send the message ‘turn right’ to the network.
- All computers in the network will see the ‘turn right’ message. If they are programmed to do so, they will flash their turning light to the right.

In a similar way, the structural messages can be transferred on the network. Small computers, dedicated to structural measurements and analysis, can be located in critical parts of the structure to measure forces, stresses, accelerations, etc. These computers can then send information to the other parts of the control

system upon request or in case of overload. Another small computer on the network, one in charge of actuator control for example, can analyse the message and reduce the actuator load.

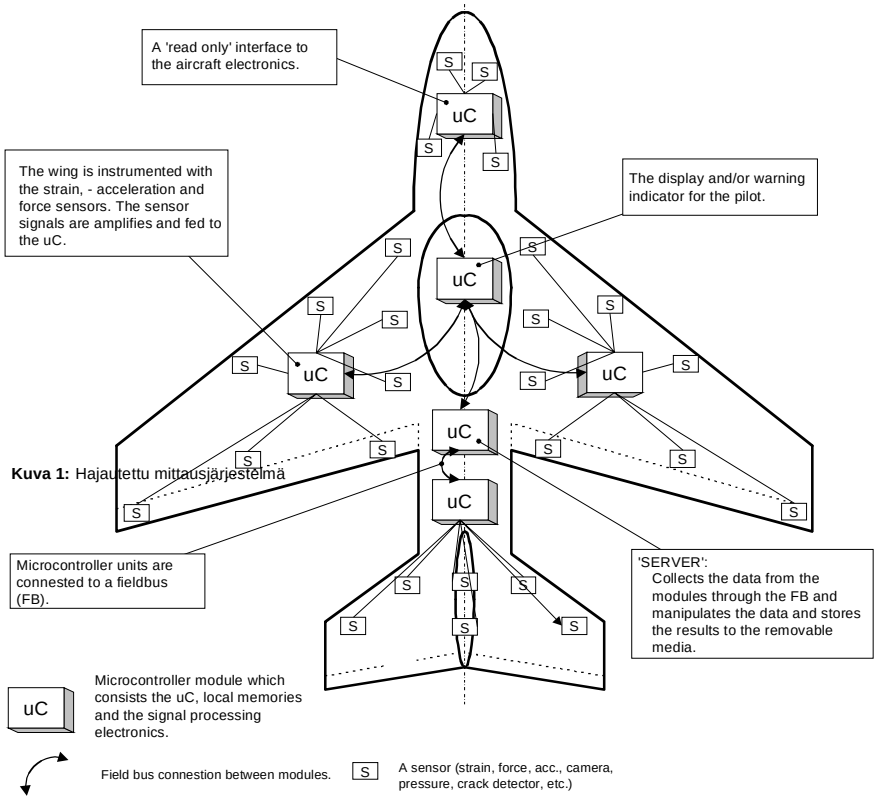

Figure 6. Distributed control and sensing system.

The CAN standard defines the physical hardware (wire between nodes, etc.) and lowest-level software to realise the message passing through the network. Protocol standards define the content and format of the data transferred through the network – its next higher-level software. In vehicle applications, one popular protocol is SAE-1939 (Society of Automotive Engineers). For specific messages not defined in the standard, SAE has defined a proprietary type of message, in which the user can define the content without harming the communication with standardised messages. This allows application-specific messages (like these structural ones) to live in harmony with traditional SAE-1939 messages. If there is danger to overload the capacity of one CAN bus with structural and traditional

messages, the bus can be multiplied. Several buses for various applications can be implemented.

5. Active fatigue damage minimisation

Control for fatigue damage minimisation includes several important areas. Those areas are mechanics of the device, measuring, monitoring that contains real-time damage detection and damage-rate calculation, decision making based on damage rate and performance of the device, and (finally) control of the device.

Minimisation of fatigue damage requires knowledge about damage rates. In addition to results of traditional measuring and monitoring, damage rate can be based on measured performance values. Measured performance values include (among others) velocity, acceleration, and temperature of the apparatus. The connection between those values and the fatigue damage rate can be formed using results from measurements and simulations.

Decision-making means the way that produces a correction for the control of the machine. This correction is a real-time solution, which is formed based on momentary damage rate and performance. The control correction minimises fatigue damage rate and simultaneously tries to maintain the highest performance of the machine. Minimising fatigue damage of the control can be accomplished in many ways. Control correction can be, for example, a coefficient that is used to modify error signals of the regulators' coefficients, or to limit the device's acceleration or its derivative.

Closed-loop control and modifiability of the control makes it easier to implement the decision-making module. Traditional closed-loop control is suitable when it is not well known how the system reacts to certain inputs. Closed-loop control measures the output of the system, compares the measured value to a desired value, and compensates for the effect of noise and changes in the system (Pyrhönen 2001). This means that control tries to track the input values that are desired and possibly accommodated with damage mitigating control. Feedback values can also be used as inputs to the intelligent decision-making process.

Control of a machine, which is complemented by the decision-making process, is an adaptive or learning process. A learning decision-making module defines a reaction method, checks and repairs its consequences, and remembers its earlier activities. An adaptive controller is a controller with transformable parameters and a parameter-adjustment method. Figure 7 presents a basic version of an adaptive system, where the Plant module is a mathematical or mechanical model of a machine. A simple damage-minimising control works just as the diagram shows. In addition to traditional feedback, there is a parameter adjustment that creates control correction. For feedback, the control correction has a set control mode (performance requirements) as input, control signal (order of performance), and output of a plant (performance, damage rate). The created corrections are parameters for damage minimising, which are adjusted in the decision-making module of the damage-minimising control.

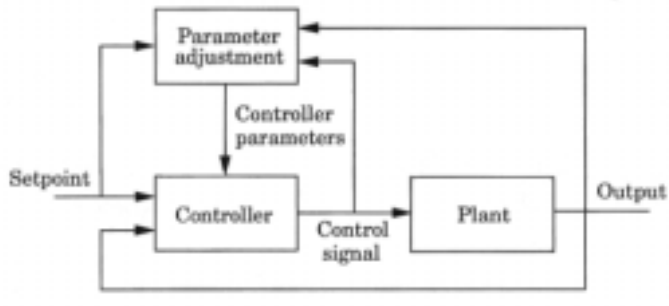

Figure 7. The flowchart of the adaptive control (Åström & Wittenmark 1995).

5.1 Tools for damage control

The reaction method produced by the decision-making procedure of the fatigue damage minimising can be direct (defined beforehand), adaptive, or learning (Figure 1). Several methods are useful for decision-making. These include, for example, neural networks, fuzzy logic, case-based reasoning, different optimisation methods, rule-based systems, and other methods that are linked to artificial intelligence. These tools can be used to estimate severity of damage and to produce control correction for damage rate minimisation. The next paragraphs present some of these methods.

Fuzzy logic consists of non-fuzzy inputs, fuzzifying, fuzzy rule base, defuzzifying, and non-fuzzy outputs. Fuzzy rule base is a group of If-Then rules. Fuzzy reasoning evaluates all the rules in parallel; after that, the results of the rules are combined together and de-fuzzified to a non-fuzzy output. Fuzzy logic was used in the demonstration simulator. Its theory and practical use is explained more in pursuance of a demonstration simulator.

Neural networks consist of neurons. Parallel neurons with inputs and outputs create a layer. A network can have one or several layers. The idea of the network is to multiply one input of the neuron by its weighting coefficient and sum that with results of other inputs of the same neuron. The level of the neuron's output depends on the sum. If the sum is over the set threshold of the neuron, then the neuron will become activated. In the case of a non-linear activation function, it is possible to increase the effectiveness of calculations by increasing the number of layers. When building the network, it is important to choose the number of layers and neurons, activation functions, feedbacks and feedforwards. The teaching of the network can be based, for example, on the desired final result and made by adjusting the weights of the network in every circuit of teaching. In this method, the teaching concentrates on the error between the output of the network and the desired output. (VTT 2001a). This kind of teaching method was used when the neural network for a fatigue-damage calculation was created for the demonstration simulator.

Case-Based Reasoning is a method that uses old example cases and solutions to solve and understand new problems. This method uses similarities found from old cases. Cases that are very similar to the actual case will be found by checking example cases through defined checking criterion. A solution to an actual case will be formed from those similar example cases. The system improves with age, when the number of example cases increase. On the other hand, using bad examples leads to errors. If there are no cases that are similar enough, the solution might not be found. This method needs a large example database. (VTT 2001b). This method is useful for decisions made by size of the crack when the structure and its behaviour are well known.

Rule-based systems present knowledge as a group of rules that informs what to do or decide in different situations. The system consists of a set of IF-THEN rules, a set of facts, and a controller for applying the rules. The forward-chaining

method starts with facts and uses rules to create new solutions. The backward-chaining method starts with a hypothesis that is attempted to be proven, and finds rules that make the hypothesis possible. (Cawsey 2001). This kind of logic, especially the forward-chaining method, might be useful when creating damage-based control correction.

Fatigue damage minimisation is an optimisation problem between damage rate and performance. Different optimisation methods will be useful when trying to obtain the right correction for the control of the system.

6. The demostration simulator

For the dynamic calculations, two different programs were used – ADAMS and Open Dynamics Engine (ODE). ADAMS is widely used in multibody system simulations, especially in the vehicle industry. ADAMS is not capable of real-time simulations, but because of its accuracy, it was used to verify results from ODE. ODE is a free C-library for making real time simulations of stiff multibody systems. Matlab/Simulink was used as a platform for the simulator.

The crane consists of a pillar, two arms, and three actuators (Figure 8). The simulator is controlled by joysticks that are connected to the Matlab/Simulink. The output values from the joysticks are the velocities of the tip of the crane, which are modified to angle velocities of the crane's joints using a program written in C. In other words, co-ordinate control works so that the user controls the tip of the crane, not the individual joints or actuators.

The C program for angle velocities also handles the crane’s operating range and limits the angle velocities when approaching the boundaries. The angle velocities are integrated to angles and transferred to a PID-controller, where they are compared to angles obtained from the dynamics module. So the PID controller controls the moments and cylinder force so that the desired angles are obtained. Besides the joint angles, the dynamics module outputs the crane's performance and stress of the first arm near the bracket.

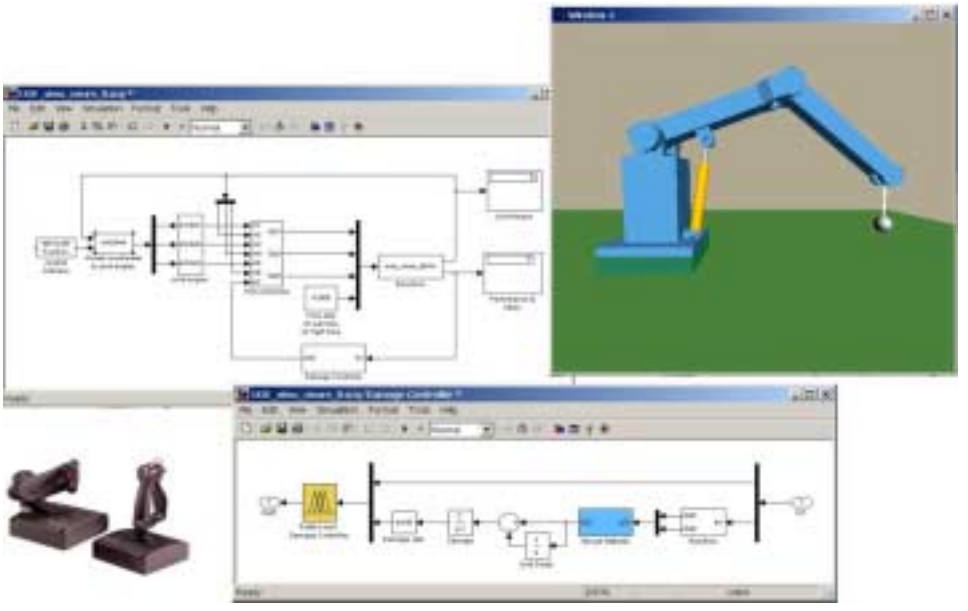

Figure 8. *The crane simulator.*

The information about damage rate is needed when you want to actively minimise the fatigue damage. It can also be used to estimate the remaining service life. The relation between performance or stress and damage rate can be described with an equation, a table, or a neural network. Damage rate based on performance parameters is probably not very accurate; stress is better. Traditionally, rainflow classification is used for stresses. The structure is damaged every time the load cycle is closed. Typically, direct observation of the damage rate will not be possible.

When actively minimising fatigue damage, you need as real-time information about the damage rate as possible. In the demonstrator, the real-time damage rate is calculated based on damage between two points on the same stress reversal (Figures 9 and 10). These points are stresses of two successive time steps.

Reference stress (O in Figure 9) is calculated using the rainflow algorithm. Reference and current stress is then transformed to stress amplitude and mean stress. These stresses then go to a neural network which calculates the damage according to the local strain method. Figures 9 and 10 show how the damage is calculated between time steps A and B. After the cycle damage (O–>B) is

calculated, it is subtracted from the cycle damage from the previous time step (O–>A). After that, the damage sum and damage rate are calculated.

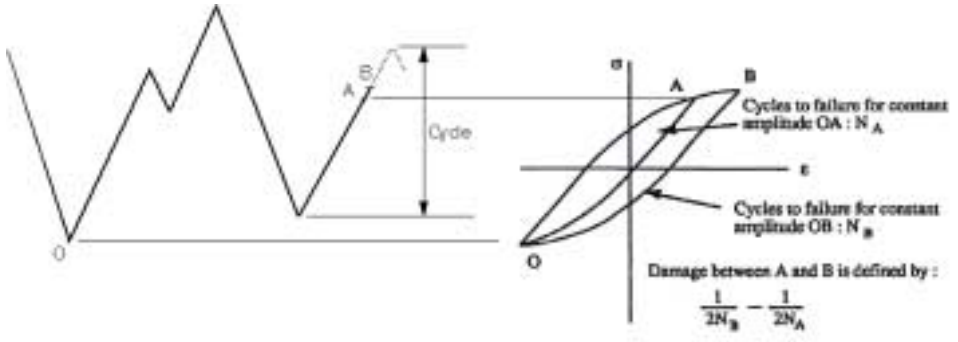

Figure 9. The damage between points A and B. (Ray et al. 1992).

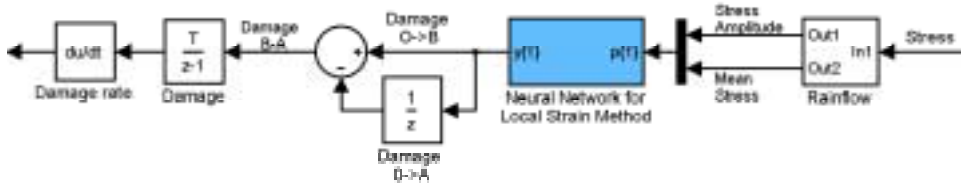

Figure 10. Simulink block for damage rate calculations.

The input values for training the damage controller's neural network were stress amplitude and mean stress level; the targets were the damage values obtained with the local strain method. The material used in the local strain method to calculate the target damages was StE 590, and the material parameters were obtained from the reference (Boller & Seeger 1987). The data set used for training the neural network was calculated using a mathcad program for the local strain method. The training data was calculated using 15 different stress amplitudes and 13 mean stress levels. Figure 11 compares the original stress-life data, lines with markers in the figure, and data calculated with the neural network. Curves are calculated using three different mean stress levels. These results are good, but better results can be obtained with a larger training data set.

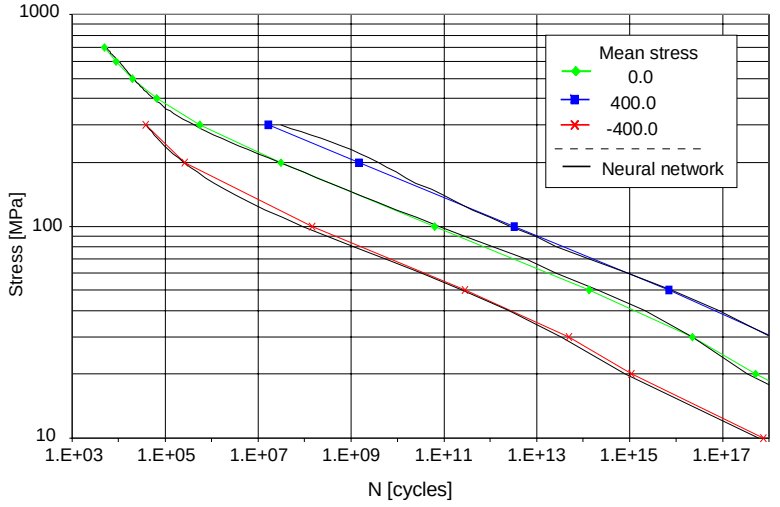

Figure 11. Comparison of original stress-life data and data calculated with neural network.

The last module of the damage controller is the fuzzy logic module that determines the *control parameters* from the *performance* and *damage rate* inputs (Figure 12). The aim is to get maximal decrease of fatigue damage rate while simultaneously maintaining the highest performance of the machine.

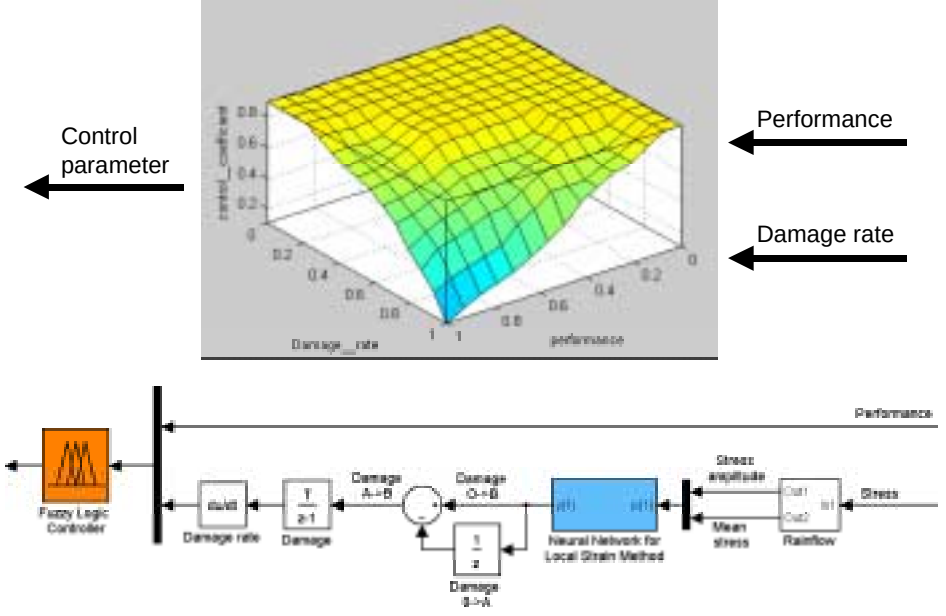

Figure 12. Fuzzy logic damage controller.

The definition range of the inputs and output was distributed into five different verbal definition areas. The data ranges of inputs and output were set to real values from 0.0 to 1.0. The shape of the membership functions was mainly triangular, except the start and end areas of the nonfuzzy data ranges. Areas of the last type had trapezoidal functions. Maximum and minimum values of membership functions were set individually as a function of nonfuzzy data range of the function in question.

Table 3 shows when the verbal definitions are fully true in the case of different membership functions. The control coefficient was set to a certain verbal value, with certain verbal values of damage rate and performance. This produces the fuzzy rule base that defines the control coefficient as a function of input variables, which is then combined through all the necessary areas of input variables. For example, if the damage rate is high and performance is in the middle, then the coefficient is high (0.7).

The fuzzy logic rule base described above was used in the demonstration simulator. The lowering of the control coefficient, which follows the growth of damage rate, was emphasised in the higher performance levels. The surface in Figure 12 presents the rule base. Minimum performance was set to 0.5, and the maximum was set to 1.0. The minimum value was chosen to get more efficient fatigue damage minimising using a minimum of performance values.

Table 3. Numerical values presenting verbal definitions as fully true, which equals to one.

Verbal definition areas of membership functions	Inputs		Output
	Damage rate	*Performance*	*Coefficient*
very low	0–>0.25	0–>0.1	0–>0.1
low	0.55	0.3	0.3
middle	0.75	0.5	0.5
high	0.9	0.7	0.7
very high	1.0	0.9	1.0

Besides *performance* and *damage rate*, there are different ways to use the fuzzy logic module and what can be used as inputs. One possibility is to use *damage* and *damage rate* inputs so that when the damage propagates, the more the fatigue is minimised (Figure 13a). In the second example, the inputs are *desired fatigue minimisation level* and *damage rate* (Figure 13b). For examples in an emergency situation, the desired fatigue minimisation level is set to zero.

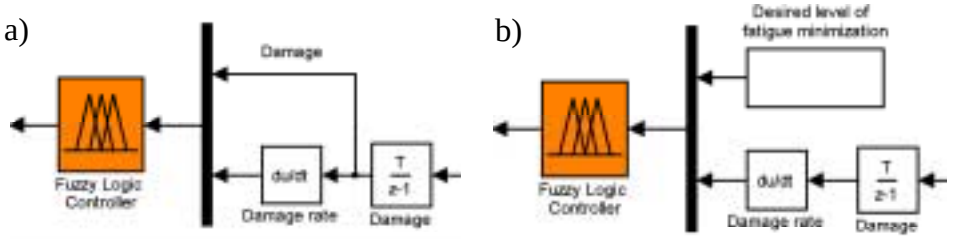

Figure 13. Fuzzy rule base as surface.

There are different ways to utilise the output of the damage controller. The *control parameter* can be used to modify factors of the PID controller, the error signal, or the acceleration rate. In this case, scaling of the acceleration rate probably gives the best results.

7. Conclusions

A machine with active fatigue durability control monitors damages or damage rates. Based on that information, it changes its behaviour. Estimated damages and damage rates are usually too conservative. In the fatigue damage minimisation, calculated estimates are very useful. With reactions based on damage observations, more drastic operation is possible. Utilisation of the active fatigue damage control offers several benefits. You can get longer service life out of your machine or, on the other hand, the structure can be lighter. When the machine knows how it can be used before and after damage occurs, accidents can be avoided. When the condition of the machine is known and the remaining service life is estimated, maintenance can be done on demand. Product development obtains more accurate information on loads, strains, and user profiles.

References

Boller, Chr. & Seeger, T. 1987. Materials data for cyclic loading. Materials science monographs, 42B, Elsevier. P. 45.

Laakso, R. & Savolainen, M. 2002 [in preparation]. Kestävyyden hallinta; Mittaustiedon käsittely. Espoo: VTT Tuotteet ja tuotanto. Tutkimusraportti BTUO33-021035.

Laakso, R., Solin, J., Pitkänen, J. & Marquis, G. 2001. Kestävyyden hallinta; Väsymisvaurion mittausmenetelmät. Espoo: VTT Valmistustekniikka. 52 p. Tutkimusraportti BVAL33-011111.

Ray, A., Wu, M., Carpino, M., Lorenzo, C. & Merril, W. 1992. Damage-mitigating control of aerospace systems for high performance and extended life. Proceedings of the 1992 American Control Conference, The Westin Hotel, Chigago, Illinois, June 24–26, 1992. New York: IEEE. Pp. 3052–3056. ISBN 0-7803-0210-9

Pyrhönen, O. 2001. Säätötekniikan perusteet. Säätötekniikan perusteet -kurssin luentomoniste. Lappeenranta: LTKK, Sähkötekniikan osasto, Sähkötekniikan laboratorio.

VTT. 2001a. Neuroverkot [www-document]. VTT Elektroniikka [referenced 7.5.2001]. Available: http://www.vtt.fi/ele/tutkimus/soh/aly/neuroverkot.htm

VTT. 2001b. Mallipohjainen diagnostiikka ja seuranta, Case-Based Reasoning – CBR [www-document]. VTT Elektroniikka [referenced 7.5.2001]. Available: http://www.vtt.fi/ele/tutkimus/soh/aly/cbr.htm

Åström, K. & Wittenmark, B. 1995. Adaptive control. Reading (MA): Addison-Wesley. 574 p. ISBN 0-201-55866-1

Published by

Series title, number and report code of publication

VTT Symposium 225
VTT–SYMP–225

Author(s)
Vessonen, Ismo (ed.)

Title

Smart materials and structures
VTT Research Program 2000–2002

Abstract

This publication documents the presentations given at the closing seminar of the "Smart Materials and Structures" (ÄLYMARA) technology program. The publication also reports the main results of the four subprojects of the research program.

The aim of the "Active materials" subproject was to gather information on available active materials and to provide support in materials issues for the other three subprojects. A state-of-the-art literature review including functional solid state, polymer and fluid materials was reported.

The purpose of the "Precision motion and force" subproject was to develop know-how to apply functional materials in the production of controlled motion and forces. Several prototype structures were designed and implemented: SMA-actuator based "finger", SMA wire-based deforming "bridge", piezo actuator-based gripper including a PC-controller system (1 MSc thesis) and a novel SMA-wire actuator concept, for which a patent has been applied.

The "Active durability control" subproject developed know-how to implement machines capable of autonomously controlling fatigue of structures. Several studies (1 MSc thesis) on active control, measurement and signal analysis techniques were reported. Functional virtual prototype with a fuzzy logic durability controller was set up and used to demonstrate the active concepts.

In the "Active vibration control" project, a test and demonstration environment was built to study adaptive control systems in active vibration control of rotors. A LicSc thesis was prepared on the basis of the promising results. Semi-active vibration control of vehicle cabins using MR fluid-based dampers and skyhook and fuzzy logic control schemes were studied. Laboratory experiments and computer simulations were used to verify the potentiality of semi-active control.

Keywords
adaptronics, smart materials, smart structures, intelligent systems, multifunctional systems, adaptive systems, vibration control, durability control, active materials, active control, semi-active control

Activity unit
VTT Industrial Systems, Otakaari 7 B, P.O.Box 13022, FIN–02044 VTT, Finland

ISBN	Project number
951–38–6278–X (soft back ed.) 951–38–6279–8 (URL: http://www.inf.vtt.fi/pdf/)	H0SU00141

Date	Language	Pages	Price
February 2003	English	100 p.	B

Name of project	Commissioned by
Smart materials and structures research program	Technical Research Centre of Finland (VTT)

Series title and ISSN	Sold by
VTT Symposium 0357–9387 (soft back ed.) 1455–0873 (URL: http://www.inf.vtt.fi/pdf/)	VTT Information Service P.O.Box 2000, FIN–02044 VTT, Finland Phone (internat.) +358 9 456 4404 Fax +358 9 456 4374

VTT SYMPOSIUM

214 10th International Symposium on Corrosion in the Pulp and Paper Industry (10th ISCPPI). Marina Congress Center, Helsinki, Finland, August 21–24, 2001. Volume 1. Ed. by Tero Hakkarainen. Espoo 2001. 370 p. + app. 2 p.

215 10th International Symposium on Corrosion in the Pulp and Paper Industry (10th ISCPPI). Marina Congress Center, Helsinki, Finland, August 21–24, 2000. Volume 2. Ed. by Tero Hakkarainen. Espoo 2001. 319 p.+ app. 2 p.

216 Puuenergian teknologiaohjelman vuosikirja 2001. Puuenergian teknologiaohjelman vuosiseminaari. Jyväskylä, 5.–6.9.2001. Toim. Eija Alakangas. Espoo 2001. 459 p.

217 Demonstrating Automated Fault Detection and Diagnosis Methods in Real Buildings. May 2001. Ed. by Arthur Dexter & Jouko Pakanen. Espoo 2001. 369 p. + app. 13 p.

218 Plant Life Management. Midterm status of a R&D project. Ed. by Jussi Solin. Espoo 2001. 268 p. + app. 9 p.

219 The Food, GI-tract Functionality and Human Health Cluster, PROEUHEALTH. 1st Workshop. Saariselkä, Finland, 1–3 February 2002. Ed. by Annemari Kuokka, Maria Saarela & Tiina Mattila-Sandholm. Espoo 2002. 65 p.

220 The 22nd Symposium on Fusion Technology Book of Abstracts. Helsinki, Finland, 9th–13th September 2002. Ed. by Seppo Tähtinen, Rauno Rintamaa, Merja Asikainen & Harri Tuomisto. Espoo 2002. 507 p.

221 Puuenergian teknologiaohjelman vuosikirja 2002. Puuenergian teknologiaohjelman vuosi-seminaari. Joensuu, 18.–19. syyskuuta 2002. Toim. Eija Alakangas. Espoo 2002. 428 s.

222 Power production from waste and biomass IV. Advanced concepts and technologies. Espoo, Finland, 8–10 April, 2002. Ed. by Kai Sipilä & Marika Rossi. Espoo 2002. 350 p.

223 Mechanics for Electronics. VTT Reasearch Programme 2000–2002. Espoo, December 4, 2002. Ed. by Pentti Eklund. Espoo 2002. 84 p.

224 Global Engineering and Manufacturing in Enterprise Networks (GLOBEMEN). Helsinki, 9.–10.12.2002. Ed. by I. Karvonen, R. van den Berg, P. Bernus, Y. Fukuda, M. Hannus, I. Hartel & J. Vesterager. Espoo 2003. 394 p.

225 Smart materials and structures. VTT Research Programme 2000–2002. Espoo, Finland, 4 th December, 2002. Ed. by Ismo Vessonen. Espoo 2003. 100 p.

226 The Food, GI-tract Functionality and Human Health Cluster, PROEUHEALTH. 2nd Workshop. Taormina, Italy, 3–5 March 2003. Toim. Annemari Kuokka, Maria Saarela & Tiina Mattila-Sandholm. Espoo 2003. 66 p.

Tätä julkaisua myy	Denna publikation säljs av	This publication is available from
VTT TIETOPALVELU PL 2000 02044 VTT Puh. (09) 456 4404 Faksi (09) 456 4374	VTT INFORMATIONSTJÄNST PB 2000 02044 VTT Tel. (09) 456 4404 Fax (09) 456 4374	VTT INFORMATION SERVICE P.O.Box 2000 FIN–02044 VTT, Finland Phone internat. +358 9 456 4404 Fax +358 9 456 4374

ISBN 951–38–6278–X (soft back ed.)
ISSN 0357–9387 (soft back ed.)

ISBN 951–38–6279–8 (URL: http://www.inf.vtt.fi/pdf/)
ISSN 1455–0873 (URL: http://www.inf.vtt.fi/pdf/)